# Microbial adaptation to long-term N supply prevents large responses in N dynamics and N losses of a subtropical forest

Xiaoge Han [a, b], Weijun Shen [a, *], Jinbo Zhang [c, d], Christoph Müller [e, f]

[a] *Center for Ecological and Environmental Sciences, South China Botanical Garden, Chinese Academy of Sciences, 723 Xingke Rd., Tianhe District, Guangzhou 510650, China*

[b] *University of Chinese Academy of Sciences, Beijing 100049, China*

[c] *School of Geography Sciences, Nanjing Normal University, Nanjing 210023, China*

[d] *Jiangsu Center for Collaborative Innovation in Geographical Information Resource Development and Application, Nanjing, 210023, China*

[e] *Department of Plant Ecology, Justus Liebig University Giessen, Heinrich-Buff Ring 26, 35392 Giessen, Germany*

[f] *School of Biology and Environmental Science, University College Dublin, Belfield, Dublin 4, Ireland*

[*] *Corresponding author: Weijun Shen (shenweij@scbg.ac.cn)*

chinaXiv:201811.00111v1

chinaXiv:201811.00111v1

**Abstract**

Atmospherically-deposited nitrogen (N) can stimulate complex soil N metabolisms and accumulations over time. Whether long-term (decadal) N deposition effects on soil N transformations and functional microbes differ from the short-term (annual) effects have rarely been assessed. Here we conducted a laboratory $^{15}N$ tracing study with soil samples from a short-term (one year) N addition site and a long-term (12 years) site in a subtropical forest. The effects of simulated N deposition on soil $N_2O$ emissions, N transformation rates and microbial nitrifying and denitrifying genes were determined. Our results showed that: (1) long-term N addition did not change soil $N_2O$ fluxes significantly in comparison to the short-term N addition. Denitrification, heterotrophic nitrification and autotrophic nitrification contributed 53%, 23% and 18% to total $N_2O$ emissions, respectively. (2) Autotrophic nitrification was the dominant N transformation process, except for the high-N treatment at the long-term site. The magnitude of soil N transformation rates was significantly different among N addition treatments but not between short- and long-term N addition sites. However, long-term N addition changed the responses of specific N transformation rates to N addition markedly, especially for the rates of nitrification, organic N mineralization to $NH_4^+$, $NO_3^-$ immobilization and dissimilatory $NO_3^-$ reduction to $NH_4^+$ (DNRA). (3) Responses of ammonia oxidizing archaea and bacteria (AOA and AOB) were stronger than denitrifying $N_2O$-producers (*nirK*) and denitrifying $N_2O$-reducers (*nosZ*) at the long-term site compared to the short-term site. (4) The close correlations among $N_2O$ flux, functional genes and soil properties observed at the short-term site was weakened at the long-term site, posing a decreased risk for N losses in the acid subtropical forest soils. There is evidence for an adaptation of functional microbial communities to the prevailing soil conditions and

in response to long-term natural and anthropogenic N depositions.

*Keywords:* Short- vs. long-term N deposition, $^{15}N$ tracing model, Gross N transformation, Net mineral N production, $N_2O$ flux, Microbial functional gene

chinaXiv:201811.00111v1

chinaXiv:201811.00111v1

## 1. Introduction

Nitrous oxide ($N_2O$) is an important greenhouse gas with stronger radiative forcing than $CO_2$ (Matson et al., 2002; Wang et al., 2014a). Terrestrial ecosystems contribute approximately 57% of the global $N_2O$ emissions (Werner et al., 2007). In particular, tropical and subtropical forests act as the largest natural terrestrial source of $N_2O$ globally (Werner et al., 2007; Cheng et al., 2014). In recent years, tropical and subtropical regions have been experiencing severe atmospheric N deposition due to the enhanced atmospheric reactive N ($N_r$) (Kanakidou et al., 2016) mainly come from anthropogenic N fertilization (MacDonald et al., 2002; Herrmann et al., 2005; Du et al., 2014; Zhu et al., 2015), biomass burning and fossil fuel combustion (Boy et al., 2008; Chen et al., 2010). The deposited inorganic and organic N are subsequently involved in soil internal N turnovers (Avrahami et al., 2002; Bai et al., 2014; Deppe et al., 2017). Forest soil $N_2O$ emissions are therefore likely affected by the increased atmospheric N deposition (Galloway et al., 2004; Galloway et al., 2008; Vet et al., 2014). However, the relationship between increased N deposition and soil N transformation/$N_2O$ emission in subtropical and tropical forests is poorly understood due to the complex interactions among various influencing factors such as climate, forest type, soil property, microbial community and land-use history (Chatskikh et al., 2005; Alm et al., 2007; Werner et al., 2007; Zhang et al., 2008; Chen et al., 2014).

Although abiotic processes such as chemodenitrification and chemical decomposition of hydroxylamine may contribute to soil $N_2O$ production (Williams et al., 1992; Bremner, 1997; Butterbach-Bahl et al., 2013), microbial nitrification and denitrification contribute over 70% of the global $N_2O$ emissions (Avrahami et al., 2002; Braker and Conrad, 2011; Butterbach-Bahl et al., 2013). Different groups of

soil microorganisms are involved in the processes of soil N transformation that produce $N_2O$ (Levy-Booth et al., 2014). For example, ammonia ($NH_3$) oxidization, the first step of autotrophic nitrification ($O_{NH4}$) that catalyzed by the *amoA*-encoded ammonia monooxygenase of ammonia oxidizing archaea and bacteria (AOA and AOB), is an important rate-limiting step for $N_2O$ production (Szukics et al., 2010; Isobe et al., 2012; Long et al., 2012; Wertz et al., 2012; Wang et al., 2014b; Tang et al., 2016). Denitrification, i.e. reduction of nitrate ($NO_3^-$) to $N_2O$ and further $N_2O$ to $N_2$ that catalyzed by several enzymes such as *narG*-encoded nitrate reductase, *nirK*/*nirS*-encoded nitrite reductase, *norB*-encoded nitric oxide reductase and *nosZ*-encoded nitrous oxide reductase, is also essential for the formation and consumption of $N_2O$ in soils (Freedman et al., 2013; Jones et al., 2013; Levy-Booth et al., 2014; Orellana et al., 2014; Yu et al., 2014; Domeignoz-Horta et al., 2017). Quantification of soil nitrifiers and denitrifiers, especially nitrifying $N_2O$-producers (AOA-*amoA*, AOB-*amoA*), denitrifying $N_2O$-producers (*nirK*/*nirS*) and denitrifying $N_2O$-reducers (*nosZ* and the newly identified $N_2O$-reducing clade), may facilitate the understanding of $N_2O$ productions and consumptions in soils (Isobe et al., 2012; Yu et al., 2014; Zhang et al., 2014; Domeignoz-Horta et al., 2015; Tang et al., 2016; Domeignoz-Horta et al., 2017; Hallin et al., 2017). Moreover, a range of environmental factors, such as soil moisture, redox potential, pH and nutrient availability, have been proved to be able to affect soil nitrifiers and denitrifiers (Bárta et al., 2010; Hu et al., 2013; Zhang et al., 2014; Zhang et al., 2015; Tang et al., 2016). Although a number of studies have been devoted to understanding the relationships among soil properties, functional microbes and $N_2O$ fluxes (Fang et al., 2008a; Yu et al., 2014; Zhang et al., 2014; Faeflen et al., 2016; Chen et al., 2017), our knowledge for the responses of microbial-regulated $N_2O$ emission to elevated N deposition in subtropical forest soils

chinaXiv:201811.00111v1

is still limited  increasing backgrounds is still limited (Avrahami et al., 2002; Zhong et al., 2015; Cui et al., 2016; Gao et al., 2016).

Soil $N_2O$ production and emission occur in diverse soil N pools via different N transformation processes, including the $N_2O$ originates from the nitrate nitrogen ($NO_3^-$-N) pool via denitrification, from the ammonium nitrogen ($NH_4^+$-N) pool via autotrophic nitrification and from the organic nitrogen ($N_{org}$) pool via heterotrophic nitrification (Müller et al., 1998; Zhang et al., 2011). Quantifying the contributions of these $N_2O$ production pathways is essential to understanding the fate of atmospherically-deposited inorganic N and organic N (Fang et al., 2008b). Since the production and consumption of $NH_4^+$ and $NO_3^-$ are also tightly associated with the mineralization of organic N to $NH_4^+$ and $NO_3^-$, the immobilization of $NH_4^+$ and $NO_3^-$ to organic N, and the dissimilatory $NO_3^-$ reduction to $NH_4^+$ (DNRA), quantifying the contributions of these processes is also crucial to uncovering the fate of atmospherically deposited N. In the last decade, progress has been made via advanced microbial and stable isotope methods to more accurately understand internal N transformations and underlying soil microbial drivers. The development of $^{15}N$ tracing techniques allows the quantification of specific N processes by differentially labelling soil N pools (e.g. $^{15}NH_4^+$ or $^{15}NO_3^-$) (Hart et al., 1994). Moreover, the atmospherically-deposited N will stimulate complex soil N metabolisms and accumulations over time (Fang et al., 2009; Wang et al., 2015; Deppe et al., 2017). The effect of N deposition over long periods of time will likely induce rate and microbial responses that are different from short-term effects. Some previous studies have addressed the temporal effects of N deposition on forest soil N transformations but mainly focused on seasonal comparisons (Breuer et al., 2000; Kiese et al., 2003; Zhu et al., 2013a); less attention has been paid to the differentiation of short-term (a

chinaXiv:201811.00111v1

couple of years) vs. long-term (over a decade) N deposition effects (Isobe et al., 2012; Gao et al., 2016; Gurmesa et al., 2016).

Subtropical forests in south China are suffering from high atmospheric N deposition (Mo et al., 2006; Zhu et al., 2013a; Zhu et al., 2015) with hitherto unknown effects on ecological processes. The Dinghushan Long-term Nitrogen Research (DHSLTNR) study (Lu et al., 2008; Liu et al., 2011) is one of the longest-running N deposition projects in China and has received 12 years of simulated N addition. This provides a unique research facility to conduct time-scale comparisons. To compare the long- vs. short-term effects of N deposition on soil N transformations and associated functional microbes, we further established a short-term N addition site that is adjacent to the long-term site. The similar hydrothermal conditions at the two sites allow the comparison of $N_2O$ emission, N transformation as well as gene regulation differences with time at different N deposition levels. Our specific objectives of the study were to: 1) quantify the relative contribution of $N_2O$ production pathways in the subtropical forest soils, 2) characterize the responsive behaviors of various N transformation processes to simulated N deposition, 3) assess the role of functional microbes in regulating $N_2O$ emission and the fate of deposited N, and 4) compared the long- vs. short-term N addition effects.

chinaXiv:201811.00111v1

## 2. Materials and methods

### *2.1 Site description and sample collection*

The simulated short-term and long-term N deposition sites are located in the

Dinghushan Biosphere Reserve (DHSBR) (23°10′ N, 112°10′ E) which belongs to Guangdong province of south China. The DHSBR covers 1155 ha, and the climate there is characterized as humid monsoon with 1927 mm mean annual precipitation. About 75% of the precipitation occurs from March to August with a distinct wet-dry seasonality. The mean annual temperature of this zone is 21.0 °C, with a minimum and maximum monthly average value of 12.6 °C in January and 28.0 °C in July (Mo et al., 2006). In addition, the reserve has experienced naturally high rates of atmospheric N deposition (20-50 kg N $ha^{-1}a^{-1}$) with total wet N deposition reaching 34.4 kg N $ha^{-1}a^{-1}$ compared to the average value of 29 kg N $ha^{-1}$ $a^{-1}$ (as inorganic N in bulk precipitation) in the 1990s (Fang et al., 2008b; Lu et al., 2013; Gurmesa et al., 2016). The two sites studied in this article are located in a monsoon evergreen broadleaf forest which has been well protected from human activities in the past 400 years (Mo et al., 2006). The soil is Ferrasols based on the World Reference Base for Soil Resources (WRB) classification system (FAO, 1998; Chen et al., 2005) with the depth ranging from 30 to 70 cm (Mo et al., 2006; Fang et al., 2009). Major tree species in this monsoon forest include *Castanopsis chinensis*, *Schima superba*, *Gironniera subaequalis*, *Syzygium acuminatissimum*, and *Aporusa yunnanensis* (Mo et al., 2006).

The field N addition experiment at the long-term site (L site) was initiated from July 2003 by spraying ammonium nitrate ($NH_4NO_3$) solution monthly (Mo et al., 2006). Four N-addition gradient treatments were set up with applications of 0, 50, 100 and 150 kg N $ha^{-1}$ $a^{-1}$ as $NH_4NO_3$. Hereafter, the four treatments are abbreviated as: control (LC), low N (LL), medium N (LM) and high N (LH), respectively. Three replicate plots (each 10 m × 20 m) were established for each N treatment (in total 12 plots). A buffer strip of about 10 m was left between adjacent plots. For each N-

chinaXiv:201811.00111v1

addition plot, the required $NH_4NO_3$ amount to the target application was dissolved in 20 L water and sprayed evenly below the canopy using a backpack sprayer (i.e. application rate of 0.1 L $m^{-2}$ was low to avoid liquid application effects) (Mo et al., 2006; Lu et al., 2013). The short-term site (S site) received N depositions from September 2014 onwards at 0, 35, 70 and 105 kg N $ha^{-1}$ $a^{-1}$ for the control (SC), low N (SL), medium N (SM) and high N (SH), respectively. Three replicates (each 15 m × 15 m, with a 10 m wide buffer strip between every adjacent two plots) under each N treatment formed 12 plots in total. $NH_4NO_3$ fertilizer was dissolved in 30 L water and sprayed evenly to N-plots (i.e. application rate of 0.1 L $m^{-2}$). At the time of soil sampling in July 2015, the long-term site and the short-term site had received simulated N deposition for approximately 12 years and one year, respectively.

Twenty-four soil samples (2 sites × 4 N treatments × 3 replicates) were collected from the surface soil (0 - 20 cm) after litter removal in July 2015. Six soil cores were randomly selected in each replicate plot and mixed into a composite sample. All soil samples were sieved (2 mm mesh) and split into three subsamples: one subsample was stored at 4 °C for the incubation studies, the second subsample was stored at -80 °C for functional gene analyses, and the third subsample was directly used or air-dried for soil physiochemical property determination, including soil water content (WC), water holding capacity (WHC), soil pH, ammonium nitrogen ($NH_4^+$-N), nitrate nitrogen ($NO_3^-$-N), total organic carbon (TOC), total nitrogen (total-N), microbial biomass carbon (MBC) and nitrogen (MBN).

### *2.2 $^{15}$N-tracing experiment*

A paired $^{15}$N tracing experiment was conducted for the collected soil samples.



chinaXiv:201811.00111v1

There were two $^{15}N$ treatments: $^{15}NH_4NO_3$ and $NH_4{}^{15}NO_3$, both at 10 atom% $^{15}N$ enrichment. For all soil samples collected from the two sites, 240, 250 ml flacks (2 $^{15}N$ treatments × 2 sites × 4 N treatments × 3 replicates × 5 sampling points) were prepared. Each flask contained fresh soil (equivalent to 20 g dry weight) and was covered by a sealing membrane with three pin-holes to allow gas exchange but avoid moisture losses. Soils were incubated in the dark at 20 °C and 40% WHC for an overnight pre-incubation. After that, 2 ml $^{15}NH_4NO_3$ or $NH_4{}^{15}NO_3$ solution was evenly added to the soil at an amount of 20 mg N $kg^{-1}$ soil (oven-dried weight), and the labelled soils were incubated in the dark at 20 °C and 60% WHC for 336 h (14 d). Gas samples were taken from the headspace of the flasks at 0.5 h (0 d), 24 h (1 d), 72 h (3 d), 168 h (7 d) and 336 h (14 d) after label addition. The incubation and gas sampling were carried out according to Zhang et al (2011). Finally, two 30-ml gases were taken from the headspace of each flask with a gastight syringe (30 mL, Ping An, China) and transferred into pre-evacuated vials (12 mL, Jing Yang, China). One gas sample was used to determine $N_2O$ concentration while the other sample was used for the analysis of $^{15}N$ enrichment in $N_2O$. After gas collection, soil samples were extracted with 2M KCl solution at a ratio of 1: 5 (soil: extractant). After KCl extraction soils were washed with distilled water to exclude inorganic nitrogen, then filtered and dried for the analysis of $^{15}N$ enrichment in organic N.

*2.3 Determination of soil properties, $N_2O$ fluxes and $N_2O$ pathways, N transformation rates and gene abundances*

*2.3.1 Soil properties*

Soil $NH_4^+$-N was measured using the Alpha-Naphthol Blue- spectrophotometer



chinaXiv:201811.00111v1

method after KCl extraction, and $NO_3^-$-N was measured using the Dual Wavelength Spectrophotometric method. Soil MBC and MBN were measured using the chloroform-fumigation-extraction method (Vance et al., 1987). Soil pH was measured using the mixture of soil/water at a ratio of 1:2.5 (m: v) by a portable pH detector (F-71G, LAQUA, HORIBA, Japan). Soil TOC was measured using the $H_2SO_4$-$K_2Cr_2O_7$-heating method. Total-N content was analyzed after $H_2SO_4$ digestion using both the Alpha-Naphthol Blue- spectrophotometer method and the Mo-Sb Anti-spectrophotometer method (Liu, 1996).

*2.3.2 N concentrations and $^{15}N$ enrichments in inorganic-N, organic-N and $N_2O$*

The $^{15}N$ enrichment of soil inorganic N ($NH_4^+$ and $NO_3^-$) in the KCl extract was measured by an isotopic ratiomass spectrometer (IRMS, Europa Scientific Integra, Crewe, UK). $^{15}NH_4^+$ and $^{15}NO_3^-$ were first separately transferred into $^{15}NH_3$ and then converted into $(^{15}NH_4)_2SO_4$ (Wang et al., 2015), while the concentrations of the two inorganic-N forms were measured by 0.005 M $H_2SO_4$ titration using a 2% $H_3BO_3$ solution as a color indicator. Briefly, the KCl extract (containing $^{15}NH_4^+$ and $^{15}NO_3^-$) was steam-distilled with magnesium oxide (MgO) for converting $NH_4^+$ to liberated $NH_3$ and the same extract in the flask was distilled again with Devarda's alloy for transferring $NO_3^-$ to liberated $NH_3$ (Feast and Dennis, 1996). The liberated $NH_3$ produced in the twice distillations was separately trapped using the boric acid solution (i.e. a titration for measuring the concentration of $NH_4^+$ and $NO_3^-$). The trapped N in the flask was then acidified by the $H_2SO_4$ solution for converting to $(NH_4)_2SO_4$. The solution after acidification was dried at 80°C for $^{15}N$ enrichment determination. After KCl extraction and filtration, the soils left were washed four times with distilled water and subsequently dried at 60 °C for the determination of organic-N concentration and

chinaXiv:201811.00111v1

$^{15}N$ enrichment. For the gas samples, $N_2O$ concentration was measured using an Agilent 7890A gas chromatograph (Agilent Technologies, Inc, USA), and the $^{15}N$ enrichment in $N_2O$ was measured using a mass spectrometer (Finnigan, MAT 253 mass spectrometer).

*2.3.3 Calculation of $N_2O$ fluxes and $N_2O$ pathway contributions*

The $N_2O$ flux in each sampling point was calculated according to standard methods (Yu et al., 2014; Xie et al., 2015) based on the $N_2O$ concentration change over time during the incubation. Based on the $^{15}N$ enrichment (atom% excess) in $N_2O$, $NH_4^+$-N, $NO_3^-$-N and also in organic-N pools in the paired $^{15}N$ tracing treatments, we calculated the contribution of different $N_2O$ emission fractions. We assumed that $N_2O$ originated from $NH_4^+$-N, $NO_3^-$-N and organic N pools via autotrophic nitrification, denitrification and heterotrophic nitrification, respectively. The contributions of these three different pathways were calculated according to the following equations (Rütting et al., 2010; Zhang et al., 2011):

$$a_{N2O} = d \cdot a_d + a \cdot a_a + h \cdot a_h \quad (1)$$

$$d + a + h = 1 \quad (2)$$

Where $a_{N2O}$ , $a_d$ , $a_a$ and $a_h$ indicate the $^{15}N$ atom% excess in $N_2O$, $NO_3^-$, $NH_4^+$, and organic N in the $^{15}NH_4^+$-labelled or $^{15}NO_3^-$-labelled treatment during the incubation; *d, a and h* indicate the $N_2O$ emission fraction that originates from the $NO_3^-$-N pool via denitrification, from the $NH_4^+$-N pool via autotrophic nitrification and from the organic N pool via heterotrophic nitrification. By inserting relevant $^{15}N$ enrichment data into the equations above we calculated the values of *d*, *a* and *h* by the back solver method in Excel (Microsoft, Inc.).

chinaXiv:201811.00111v1

To understand $^{15}N$ losses from the labelled inorganic N pools in form of $N_2O$, we calculated the percentage of the $^{15}N$ enrichment (atom% excess) in $N_2O$ to the $^{15}N$ enrichment in the $NH_4^+$-N pool, i.e. $^{15}N_2O/^{15}NH_4^+$% in the $^{15}NH_4^+$-labelled treatment, and also the percentage of the $^{15}N$ enrichment in $N_2O$ to the $^{15}N$ enrichment in the $NO_3^-$-N pool, i.e. $^{15}N_2O/^{15}NO_3^-$% in the $^{15}NO_3^-$-labelled treatment for each sampling point of the incubation.

*2.3.4 Quantification of N transformation rates*

Gross N transformation rates were quantified by a $^{15}N$ tracing model (Müller et al., 2007) (Fig S1). The model considered ten transformation processes related to the turnover of organic N and inorganic N in soil: (1) $M_{Nrec}$, mineralization of recalcitrant organic N to $NH_4^+$; (2) $I_{NH4\text{-}Nrec}$, immobilization of $NH_4^+$ to recalcitrant organic N; (3) $M_{Nlab}$, mineralization of labile organic N to $NH_4^+$; (4) $I_{NH4\text{-}Nlab}$, immobilization of $NH_4^+$ to labile organic N; (5) $O_{Nrec}$, oxidation of recalcitrant organic N to $NO_3^-$ (heterotrophic nitrification); (6) $I_{NO3}$, immobilization of $NO_3^-$ to recalcitrant organic N; (7) $O_{NH4}$, oxidation of $NH_4^+$ to $NO_3^-$ (autotrophic nitrification); (8) $D_{NO3}$, dissimilatory $NO_3^-$ reduction to $NH_4^+$ (DNRA); (9) $A_{NH4}$, adsorption of $NH_4^+$ on cation exchange sites; (10) $R_{HN4a}$, release of absorbed $NH_4^+$. The tracing model calculated these N transformation rates based on the concentration and $^{15}N$ enrichment values (average ± standard deviations) of inorganic N and organic N from the two distinct $^{15}N$ labelled treatments during the experimental duration. Finally, N transformation rates of all the eight N addition treatments at the two sites were calculated over the 14 d period and expressed in units of mg N $kg^{-1}$ soil $day^{-1}$.

Based on the results from the $^{15}N$ tracing model we calculated net $NH_4^+$ production rates ($NET_{NH4prod.}$) and net $NO_3^-$ production rates ($NET_{NO3prod.}$):

chinaXiv:201811.00111v1

$$NET_{NH4prod.} = M_{Nrec} + M_{Nlab} + R_{NH4a} + D_{NO3} - I_{NH4-Nrec} - I_{NH4-Nlab} - A_{NH4} \quad (3)$$

$$NET_{NO3prod.} = O_{Nrec} + O_{NH4} - I_{NO3} - D_{NO3} \quad (4)$$

*2.3.5 Soil DNA extraction and functional gene abundance quantification*

DNA was extracted from 0.25 g fresh soil (before incubation) using PowerSoil® DNA Isolation kit (ANBIOSCI TECH LTD) following the manufacturer's instructions. The extracted DNA solution was checked for quantity and quality using a Nanodrop spectrophotometer (NanoDrop Technologies Inc., Wilmington, DE). Meanwhile, AOB-*amoA* and AOA-*amoA* were chosen to represent nitrifying community groups, *nirK* and *nosZ* were chosen to represent denitrifying community groups. The primers of four genes are listed in Table S1 based on previous studies (Rich et al., 2003; Levy-Booth et al., 2014).

Quantitative PCR was carried out with an ABI 7500 CFX96 Optical Real-Time Detection System (Bio-Rad Laboratories, Inc., Hercules, CA) by using SYBR green kits. The 20 μL reaction mixture contains 10 μL SYBR Premix Ex Taq (Tli RNaseH Plus, Takara Biotechnology, Japan), 0.4 μL Forward Primer, 0.4 μL Reverse Primer, 0.4 μL Rox Reference Dye II (Takara Biotechnology, Japan), 2 μL DNA template and 6.8 μL dd$H_2O$. Standard curves were obtained by serially diluting ($10^{-2}$ - $10^{-9}$ copies $\mu l^{-1}$) already quantified plasmid DNA containing the AOB-*amoA*, AOA-*amoA*, *nirK* or *nosZ* gene fragment. The standard plasmids were prepared from the extracted DNA samples using same primers as above. The PCR amplification efficiency - $R^2$ was 103.0% - 0.997 for AOB-*amoA*, 101.0% - 0.982 for AOA-*amoA*, 99.8% - 0.980 for *nirK* and 95.3% - 0.994 for *nosZ*. Gene reaction programs were listed in Table S2 based on previous studies (Rich et al., 2003; Levy-Booth et al., 2014).

chinaXiv:201811.00111v1

*2.4 Statistical analyses*

One-way ANOVA analyses followed by least significant difference (LSD) tests were used to test the significant differences of soil properties, $N_2O$ emission rates, gross N transformation rates and functional gene abundances among different N addition levels at each site. Two-way ANOVA analyses were performed to compare the difference of $N_2O$ fluxes, N transformation rates and gene abundances between the short-term and long-term sites. Two pairs of N addition levels at the short-term site (SL: 35 kg N $ha^{-1}$ $a^{-1}$; SH: 105 kg N $ha^{-1}$ $a^{-1}$) and the long-term site (LL: 50 kg N $ha^{-1}$ $a^{-1}$; LM: 100 kg N $ha^{-1}$ $a^{-1}$) were compared correspondingly. Before one-way and two-way ANOVAs, data normality was tested and logarithmic transformation was applied if necessary. To quantitatively compare the N addition effects between the two sites, we also calculated the relative change percentage (%) of soil $N_2O$ fluxes, N transformation rates and gene abundances under N addition treatments to those under the control treatment. Moreover, Pearson correlation analyses (SPSS 17.0, SPSS Inc., Chicago, USA) were conducted to detect the relations among soil properties, gene abundances and $N_2O$ fluxes for both sites. Statistically significant differences were analyzed for $P < 0.05$ values unless otherwise stated. All statistical analyses were performed in SPSS 17.0 (SPSS Inc., Chicago, USA).

**3. Results**

*3.1 Background soil chemical properties at the short- and long-term sites*

Soils from both sites were strongly acidic with average pH of 3.8 at the long-term



chinaXiv:201811.00111v1

site and that of 3.9 at the short-term site ($p < 0.05$, Table S3). Soil $NO_3^-$-N concentration was significantly higher than $NH_4^+$-N concentration in the soils for both sites, while the short-term site had a relatively lower $NO_3^-$-N content compared to the long-term site. The long-term site soils also had relatively higher TOC content ($p < 0.05$) and higher total-N content than the short-term site soils (Table S3). No significant difference for the C/N ratio was found among the four N treatments within each site and between the two sites ($p > 0.05$, Table S3).

*3.2 N concentrations and $^{15}N$ enrichments in inorganic-N and $N_2O$*

During the 14 days of tracing incubation, soil $NH_4^+$ concentration decreased on average by 7.7% and by 15.5% across the four N treatment levels for the short- and long-term sites, respectively; whereas soil $NO_3^-$ concentration increased on average by 25.0% and 10.2% for the short- and long-term sites, respectively (Fig. S2a, b, d, e). A decline in the $^{15}N$ enrichment of the $NH_4^+$-N pool was observed when ammonium was labelled (Fig. S2c), indicating that natural abundance or low abundance of $NH_4^+$ entered this pool. A similar declining trend was observed in the $^{15}N$ enrichment of the $NO_3^-$-N pool when nitrate was labelled (Fig.S2f), showing natural or low abundance of $NO_3^-$ entered the pool. Furthermore, the $^{15}N$ enrichment of the $NO_3^-$-N pool increased in the ammonium labelled treatment (Fig. S2c), indicating a conversion of labelled $NH_4^+$ to $NO_3^-$ (e.g. ammonia oxidation). The modelled and observed data agreed well with the $R^2$ being generally larger than 0.92.

The $^{15}N$ enrichment in $N_2O$ ranged from 0.01 to 0.53 atom% excess during the incubation, and showed initially an increase followed by a decreasing trend towards the end of the incubation (14 d) (Fig. 1a, c). In addition, $N_2O$ emitting from the nitrate



chinaXiv:201811.00111v1

labelled soils showed a significantly higher $^{15}N$ enrichment than $N_2O$ emitting from the ammonium labelled soils during the incubation ($p < 0.05$, Fig. 1a, c). A significantly higher $^{15}N_2O/^{15}NO_3^-$% was found compared to the $^{15}N_2O/^{15}NH_4^+$% throughout the whole incubation (Fig. 1b, d).

*3.3 $N_2O$ fluxes and production pathways*

With increase in the level of N addition, soil average $N_2O$ fluxes of the low or medium N treatments during the incubation also increased, while $N_2O$ fluxes of the high N treatments decreased at the two sites (Fig. 2a). The $N_2O$ flux in SL, SM and SH was 42.3%, 2.7% higher and 11.6% lower than the treatment control (SC) at the short-term site, while the $N_2O$ flux in LL, LM and LH was 35.7%, 378.5% and 106.7% higher than the control (LC) at the long-term site. Except for the significantly higher flux in LM, $N_2O$ fluxes were not significantly different among N treatments or between sites ($p > 0.05$). As to $N_2O$ emission pathways, denitrification (d) contributed more than 40% to soil $N_2O$ production, while the trend of this pathway within increasing N levels differed at the two sites (short-term: SC<SH<SL<SM; long-term: LL<LM<LC<LH) (Fig. 2b). The contribution of heterotrophic (h) and autotrophic nitrification (a) was in a range of 17.7% - 36.8% and 14.3 - 23.2%, respectively. However, the two nitrification fractions of $N_2O$ differed at the short- vs. long-term within increasing N levels (h, short-term: SM<SC<SL<SH, long-term: LC<LH<LM<LL; a, short-term: SL<SH<SM<SC, long-term: LM<LL<LH<LC) (Fig. 2b). Furthermore, the contribution of different $N_2O$ emission fractions changed from a dominant heterotrophic nitrification ($N_2O_h$) to denitrification ($N_2O_d$) towards the end of the study, while the contribution of autotrophic nitrification ($N_2O_a$) increased in the

chinaXiv:201811.00111v1

early stage (0 - 7d) of the incubation (Fig. 2c). The contribution of the three fractions was on average 53% (d), 28% (h) and 18% (a) during the incubation, showing an overall dominance of denitrification in the studied subtropical forest soils (Fig. 2c).

*3.4 Gross and net N transformation rates*

Gross autotrophic nitrification rate ($O_{NH4}$) was highest among all the ten N transformation rates under almost all N treatments, followed by gross mineralization rates of recalcitrant and labile organic N to $NH_4^+$ ($M_{Nrec}$ and $M_{Nlab}$) (Table S4). Gross heterotrophic nitrification rate ($O_{Nrec}$) was much lower than gross autotrophic nitrification rate in the studied subtropical forest soils (Table S4). Total gross nitrification rate ($O_{NH4} + O_{Nrec}$, not shown in the table) ranged from 0.08 mg $kg^{-1}$ $d^{-1}$ to 0.19 mg $kg^{-1}$ $d^{-1}$ while $O_{NH4}$ contributed over 99% to the total $NO_3^-$ production. Except for SC and LH treatments, soil gross $NO_3^-$ immobilization rate ($I_{NO3}$) was higher than gross $NH_4^+$ immobilization rates ($I_{NH4\text{-}Nres}$, $I_{NH4\text{-}Nlab}$) and gross rates of dissimilatory $NO_3^-$ reduction to $NH_4^+$ (DNRA) ($D_{NO3}$) under most N treatment conditions (Table S4), indicating that $NO_3^-$ was more easily trapped in the organic N pool than in the $NH_4^+$-N pool. Net $NO_3^-$ production rate ($NET_{NO3prod.}$) was much higher than net $NH_4^+$ production rate ($NET_{NO3prod.}$), while LH had the highest net $NH_4^+$ loss but the lowest net $NO_3^-$ production from all the eight N treatments. $NET_{NO3prod.}$ also differed significantly among the four N-treatments in either the short-term or the long-term site ($p < 0.05$). All the ten gross N transformation rates considered in both sites were statistically different with respect to the N treatments ($p < 0.05$, Table S4). However, according to two-way ANOVA results, long-term N addition did not significantly change N transformation rates in soils ($p > 0.05$) in

chinaXiv:201811.00111v1

comparison to the short-term site.

The response direction of gross organic N mineralization rates ($M_{Nlab}$ and $M_{Nrec}$) to N addition was opposite between short-term and long-term sites (Fig. 3a, b), so did the gross rate of heterotrophic nitrification ($O_{Nrec}$) (Fig. 3e). Gross mineralization rate of labile organic N to $NH_4^+$ ($M_{Nlab}$) was 82%, 144% and 58% higher respectively in SL, SM and SH than that in SC at the short-term site, but the $M_{Nlab}$ was 44%, 20% and 47% lower respectively in LL, LM and LH than that in LC at the long-term site (Fig. 3a). In contrast, the gross mineralization rate of recalcitrant organic N to $NH_4^+$ ($M_{Nrec}$) was 49%, 16% and 15% lower respectively in SL, SM and SH than that in SC at the short-term site, whereas the $M_{Nrec}$ was 51%, 85% and 128% higher respectively in LL, LM and LH than that in LC at the long-term site (Fig. 3b). The large stimulation effect of N addition on the gross rates of $NO_3^-$ immobilization ($I_{NO3}$) and dissimilatory $NO_3^-$ reduction to $NH_4^+$ (DNRA) ($D_{NO3}$) at the short-term site, decreased or even became inhibition at the long-term site (Fig. 3d, f). Compared with the short-term site, the high N addition treatment at the long-term site induced the largest inhibition effect on the gross autotrophic nitrification rate ($O_{NH4}$) and the net $NO_3^-$ production rate ($NET_{NO3\text{-}prod}$) (Fig. 3c, g).

*3.5 Functional gene abundance*

AOA-*amoA* was the most abundant, followed by *nirK*, *nosZ* and AOB-*amoA*, while AOB-*amoA* was least abundant at both the short-term and long-term sites (Fig.4 a, b, d, e). The ratio between denitrifying and nitrifying gene abundance, i.e. (*nirK* +*nosZ*)/(AOB-*amoA* + AOA-*amoA*) was mostly less than 1.0 at both sites (Fig. 4c), indicating that nitrifiers were more abundant than denitrifiers in the forest soil. The



chinaXiv:201811.00111v1

*nosZ*/*nirK* ratio was mostly less than 1.0 at both sites (Fig. 4f), indicating that $N_2O$-producers were less abundant than $N_2O$-reducers. Although AOA-*amoA*, *nirK* and (*nirK* +*nosZ*)/(AOB-*amoA* + AOA-*amoA*) ratio responded significantly to N addition within each site ($p < 0.01$) (Fig. 4b, c, d), the abundance of all assessed functional genes showed no significant difference between the two sites ($p > 0.05$).

Similar stimulation effects of N addition on *nirK* abundance were observed at the two N addition sites (Fig. 4d, inset). Except the high N treatments of the two sites, the direction of *nosZ* abundance, (*nirK* +*nosZ*)/(AOB-*amoA* + AOA-*amoA*) and *nosZ*/*nirK* ratios was also the same (Fig. 4 c, e, f, insets), indicting a stimulation effect caused by low and medium N additions in the forest soil. However, except the high N treatments of the two sites, the direction of AOB-*amoA* abundance response to N addition was opposite between the two sites (Fig. 4a, inset). The abundance of AOA-*amoA* was 26.5% lower, 72.0% higher and 127.3% higher respectively in SL, SM and SH than that in SC at the short-term site, while the AOA-*amoA* abundance was 46.8% lower, 8.0% higher and 27.7% lower respectively in LL, LM and LH than that in LC at the short-term site (Fig. 4b, inset), indicating that under high N treatment the AOA-*amoA* abundance was stimulated at the short-term site but suppressed at the long-term site.

### *3.6 Correlations among soil properties, abundance of functional genes and $N_2O$ fluxes*

The correlation relations among soil properties, functional gene abundance and $N_2O$ fluxes differed between short-term and long-term sites (Fig. 5). At the short-term site, soil $N_2O$ flux was positively correlated with *nosZ* abundance ($p < 0.05$). The



chinaXiv:201811.00111v1

abundance of *nosZ* was also positively correlated with both *nirK* ($p < 0.05$) and AOB-*amoA* abundances ($p < 0.01$), implying there might exist possible interactions between nitrifying and denitrifying groups in regulating $N_2O$ emission. AOA-*amoA* abundance was negatively correlated with soil pH ($p < 0.01$) but positively with soil C/N ratio ($p < 0.05$) (Fig. 5). The abundance of AOB-*amoA* and *nosZ* was positively correlated with soil $NH_4^+$-N, total N and C/N ratio ($p < 0.05$) (Fig. 5), indicating that nitrifying $N_2O$-producers and denitrifying $N_2O$-reducers were also linked to substrate availability in the acid soil environment. Positive correlations were also found between (*nirK* +*nosZ*)/(AOB-*amoA* + AOA-*amoA*) ratio and soil $NH_4^+$-N and between *nosZ*/*nirK* ratio and TOC (Fig. S3a), further indicating that the composition of nitrifiers and denitrifiers could possibly be affected by soil substrate availability. However, at the long-term N addition site, positive correlations were only found between $N_2O$ flux and AOA-*amoA* abundance ($p < 0.05$), and between AOB-*amoA* abundance and pH ($p < 0.05$) (Fig. 5). In general, the correlations among soil properties, functional gene abundance and $N_2O$ fluxes was tighter at the short- than the long-term site.

chinaXiv:201811.00111v1

## 4. Discussion

### *4.1 Responses of $N_2O$ fluxes and $N_2O$ production pathways to short- and long-term N additions*

The stimulation effect of N addition on $N_2O$ emission rates was obvious only in the low and medium N treatments at the two sites (Fig. 2a). The $N_2O$ production-consumption balance (Xu et al., 2012; Zhang et al., 2014) during the denitrification

process of the forest soil may be changed: low and medium N additions favored $N_2O$ production but not $N_2O$, whereas this effect became weaker under high N addition. The more dominant $N_2O$ production than consumption is also reflected by the more abundant $N_2O$-producer (*nirK*) than $N_2O$-reducer (*nosZ*) (Fig. 4 d, e, f), which implied a higher activity of *nirK* than *nosZ* in the subtropical forest soil (Zhang et al., 2014). However in the high N treatments, $N_2O$ emissions were reduced at the short-term site but still stimulated at the long-term site compared to the controls (Fig. 2a). This is in contrast to the results from a montane forest with 3-4 years of N addition compared to 11-12 years N addition of a lowland forest (Corre et al., 2014). Possible reasons might be that soil microbes responsible for $N_2O$ emissions were more sensitive in responding to short-term and higher N additions, but gradually adapted over longer time periods, so that the stimulation effect at high-N subsided. Although long-term N addition did not induce significant changes in total $N_2O$ emission, the contribution of the various emission pathways changed, with higher denitrification contribution (53%) and lower heterotrophic (28%) and autotrophic nitrification contributions (18%) (Fig. 2b). Thus denitrification remained the dominant pathway for $N_2O$ emissions in this subtropical forest soil, which is consistent with the conclusion of Zhang et al. (2011). The $^{15}N_2O/^{15}NH_4^+$% and $^{15}N_2O/^{15}NO_3^-$% were not significantly different among increasing N levels or between short-term and long-term sites (Fig. 1b, d). This is not in line with previous findings which showed that increasing ammonium concentrations supported a higher contribution of nitrification to $N_2O$ production (Müller et al., 1998; Avrahami et al., 2002). Possible reasons might be that the top soils from this subtropical forest had been naturally N-saturated in the control treatments (SC and LC) (Gurmesa et al., 2016), thus causing a non-recognizable response of the nitrification or denitrification contribution to additional $NH_4^+$ or $NO_3^-$.

chinaXiv:201811.00111v1

By combining our observed N rate dynamics, we suspect that the added $NH_4^+$ in the forest soil was quickly transformed into $NO_3^-$, and subsequently denitrified into gaseous N ($N_2O$). This coupled nitrification-denitrification process is prevalent when rates of autotrophic nitrification are high and may have contributed to the low contribution of nitrification related $N_2O$ (Müller et al., 2014). This process may also contributed to the significantly lower $^{15}N$ enrichment in $N_2O$ in contrast to the higher $^{15}N$ enrichments in $NH_4^+$ and $NO_3^-$ in the subtropical forest soil (Fig. 1a, c; Fig. S2 c, f).

We separately labelled the $NH_4^+$-N pool and $NO_3^-$-N pool in the paired $^{15}N$ tracing incubation. The $^{15}N$ enrichment in $NO_3^-$ was higher than the $^{15}N$ enrichment in $N_2O$ in the $^{15}NH_4^+$-labelled treatment. The $^{15}N$ enrichment in $NH_4^+$ was also higher than the $^{15}N$ enrichment in $N_2O$ in the $^{15}NO_3^-$-labelled treatment (Fig. S2). This further implies that the transformation from $NH_4^+$ to $NO_3^-$ was more prevalent than the transformation from inorganic N to $N_2O$. Autotrophic nitrification only contributed 18% to the total $N_2O$ flux, despite the dominant status of this process in the ten N transformation processes which supports the above reasoning. This may indicate that fast autotrophic nitrification induced $N_2O$ production may also have stimulated further $N_2O$ reduction to $N_2$, possibly via nitrifier-denitrification (Müller et al., 2014). Thus, the measurement of $N_2$ and its $^{15}N$ enrichment would further elucidate this possible process. Heterotrophic nitrification contributed considerably (28%) to $N_2O$ fluxes while only a tiny part (1%) contributed to total $NO_3^-$ production (Table S4, Fig. 2c). This could be explained by the "hole-in-the-pipe" model and $N_2O$ gas leakage characteristics in subtropical forest soils: the higher autotrophic nitrification rate induced a bigger "hole" for $N_2O$ leakage while the lower heterotrophic nitrification rate induced a smaller "hole" for $N_2O$ leakage, thus

chinaXiv:201811.00111v1

inducing the comparability of the two $N_2O$ production pathway contributions (Firestone and Davidson, 1989; Zhang et al., 2014).

*4.2 Responses of soil N transformation rates to short- and long-term N additions*

Except for the high N treatment at the long-term site, the subtropical forest soil which received both natural (SC, LC) and anthropogenic N depositions showed higher gross autotrophic nitrification and mineralization rates than other N transformation rates (Table S4). According to Cheng et al. (2014), the relative fast transformations from $NH_4^+$ to $NO_3^-$ and from organic N to $NH_4^+$ might be one of the reasons for the natural N enrichment in the humid subtropical forest soil. Moreover, the more dominant autotrophic nitrification than mineralization processes (except for the high N treatment at the long-term site) also well explains the higher $NO_3^-$ than $NH_4^+$ concentrations in the forest soil (Table S3). The particularly higher gross $NH_4^+$ immobilization rates ($I_{NH4\text{-}Nrec}$, $I_{NH4\text{-}Nlab}$), higher gross mineralization rates ($M_{Nrec}$) but lower gross autotrophic nitrification rates ($O_{NH4}$) in the long-term high N treatment (LH) (Table S3) suggest that the soil mineralization-immobilization turnover (MIT) became more dominant than $NH_4^+$-$NO_3^-$ turnover (i.e. autotrophic nitrification) after long-term anthropogenic N addition. In addition, the significant differences of soil N transformation rates among N treatments at both sites (Table S4) further strengthens the implication importance of N transformation responses for the N enrichment, N loss and soil acidification in subtropical forest ecosystems (Gao et al., 2015). However, N transformation rates were not different significantly between the short-term and long-term sites (Table S4). Previous results revealed that soil N transformation rates are affected by a series of factors, including the interacted N

chinaXiv:201811.00111v1

transformation processes (nitrification-mineralization, mineralization-immobilization), soil microbes (microbial activity and functional abundances) and soil properties (C/N ratio, TOC and pH) (Bengtsson et al., 2003; Zhu et al., 2013b; Gao et al., 2015; Chen et al., 2017). So the insignificant change of soil N transformation rates at the long-term site might be owed to that, although long-term anthropogenic N addition still induced significant changes in soil N transformation rates, the interacted soil microbes which play roles in N transformation processes have adapted to current soil conditions. The combined effects of diverse soil abiotic and biotic factors on N transformations were weakened, thus finally preventing the possibly large responses of N transformations to prolonged N addition.

Our results showed that the rate responses of specific N transformation processes, which mainly associate to the fate of $NH_4^+$ and $NO_3^-$, were different between the short- and long-term sites (Fig. 3). Previous studies have revealed that soil organic matter fractions are linked to different functional microbes while their responses to N depositions are also different (Frey et al., 2004; Cusack et al., 2011). So the quantification of the gross mineralization rates of labile organic N ($M_{Nlab}$) and recalcitrant organic N ($M_{Nrec}$) will facilitate the understanding of the fast (labile organic N) and slow (recalcitrant organic N) turnover of soil organic N pools, respectively (Gao et al., 2016). In our study, $M_{Nlab}$ was stimulated by short-term N addition but was inhibited by long-term N addition, while results in $M_{Nrec}$ are totally opposite (Fig. 3a, b insets), showing different response directions of gross mineralization rates not only between labile and recalcitrant organic N forms but also between short- and long-term N addition treatments. Possible reasons might be that, short-term N addition limited the biomass and activity of the soil fungi which participant into the mineralization of recalcitrant organic N, thus indirectly inducing



chinaXiv:201811.00111v1

an inhibition in $M_{Nrec}$ (Frey et al., 2004; Schimel and Bennett, 2004). Moreover, N addition may also enhance the transformation of soil labile organic matter to recalcitrant organic matter (Maaroufi et al., 2015). This might be one of the reasons for the stimulated $M_{Nlab}$ but the inhibited $M_{Nlab}$ by short-term N addition. The stimulation effect of long-term N additions on $M_{Nrec}$ might be owed to that, the microbial N limitation was alleviated after long-term N addition, thus inducing an increased microbial activity for the stimulation of organic matter decomposition (Koranda et al., 2014; Gao et al., 2016). The inhibited $M_{Nlab}$ at the long-term site might be a downregulation response to the microbial upregulation to $M_{Nrec}$, while the opposite responses in $M_{Nrec}$ and $M_{Nlab}$ under N additions could be contributed by the changed stabilization of soil organic matter into recalcitrant compounds, and also by the changed microbial extracellular enzyme activity which conduct the production and decomposition of soil organic compounds (Sinsabaugh et al., 2005; Janssens et al., 2010; Gao et al., 2016). The response of soil gross autotrophic nitrification rate was most significant, except for the high N treatment of the long-term site (Fig. 3c inset), indicating that under this highest N addition rate (i.e. 150 kg N $ha^{-1}$ $a^{-1}$), soil may have changed most and thus contributed much less to nitrifying $N_2O$ emission. The special change of soil in the high N treatments of the long-term site could also be reflected by the lowest net $NO_3^-$ production rate and the highest $NH_4^+$ immobilization rate in comparison to other N treatments (Table S4). Soil gross heterotrophic nitrification rate ($O_{Nrec}$) was stimulated by short-term N addition but was inhibited by long-term N addition (Fig. 3d), implying that the production of $N_2O$ and $NO_3^-$ via heterotrophic nitrification pathways tented to increase at the short-term but decrease at the long-term site. The more positive responses of $O_{Nrec}$, $I_{NO3}$ and $D_{NO3}$ at the short-term than long-term site prevent a higher loss risk of soil $NO_3^-$ through gaseous N emission

chinaXiv:201811.00111v1

(denitrification) (Wang et al., 2015).

*4.3 Regulations of soil nitrifiers and denitrifiers in $N_2O$ emissions and their abiotic controllers*

Previous study exhibited higher abundance of ammonia-oxidizing archaea (AOA) in the same subtropical forest which is consistent with our present finding (Isobe et al., 2012). Moreover, several studies have highlighted a predominant role of AOA in nitrification (Gubry-Rangin et al., 2010; Verhamme et al., 2011; Zhang et al., 2012; Faeflen et al., 2016). So the dominant autotrophic nitrification in our current results (Table S4) might be explained by the more abundant AOA than AOB in the strong acidic soil (Zhang et al., 2012; Faeflen et al., 2016). For a better defining the relative importance of AOA and AOB in the nitrification processes, future explorations of the archaeal and bacterial ammonia oxidizer communities needs to be considered (Gubry-Rangin et al., 2010). Functions of *nirK* and *nosZ* in relationship to denitrification processes have proved to be different: *nirK* plays roles in $N_2O$ production while *nosZ* play roles in $N_2O$ reduction or consumption (Zhang et al., 2014; Domeignoz-Horta et al., 2017). Our results revealed a slightly higher abundance of *nirK* than *nosZ* (Fig. 4d, e, f), potentially indicting that $N_2O$ production exceeds $N_2O$ reduction and further contributing to $N_2O$ emission out of the forest soil. This is also in line with previous findings that the studied subtropical forest soil plays as a natural source of $N_2O$ (Fang et al., 2008a; Tang et al., 2006). However, it is worth mentioning that NO as another intermediate of denitrification cannot be neglected in considering gene regulation functions since *nirK* plays essential roles in the second step of denitrification, i.e. nitrite reduction to NO (Levy-Booth et al., 2014). Moreover, *nirS* as another

chinaXiv:201811.00111v1

molecular marker gene of denitrifying bacteria for this step still needs to be fully understood (Prieme et al., 2002; Bárta et al., 2010). The *nosZ*/*nirK* ratio in most N treatments was less than 1 (Fig. 4f) and finally led to an average value of 0.68 (data not shown) without considering the effects of N addition. This is dramatically opposite with the findings of Zhang et al. (2014) which uncovered an average value of 0.7 for *nirK*/*nosZ* ratio in subtropical soils. Possible reasons might be that, the strong acidic as well as highly weathered soil in our subtropical forest contributes to a higher redox potential, which supports a more active *nirK* than *nosZ* communities in the soil (Qafoku et al., 2004; Xu and Cai, 2007; Zhang et al., 2014).

Compared with the short-term N site, the prolonged N addition at the long-term site did not induce significant changes in functional gene abundances, but changed the responses of specific functional gene abundances to N addition treatments markedly (Fig. 4). This further highlights a higher importance of functional gene response patterns to N addition levels than gene responses to N addition durations. Possible reasons for the insignificant changes of gene abundances under the long-term N additions might be that, the activity of soil nitrifiers and denitrifiers are affected by soil abiotic conditions to a large extent, including pH, redox potential, N availability and other nutrients (Avrahami et al., 2002; Bárta et al., 2010; Hu et al., 2013; Yu et al., 2014; Zhang et al., 2014). Thus the comprehensive effects of soil abiotic factors eliminated possibly significant responses of functional groups with the N addition duration prolong. We observed significant responses of AOA-*amoA* and *nirK* abundances but not AOB-*amoA* or *nosZ* abundances to N addition treatments at the two sites (Fig. 4). This suggests different response sensitivities of soil functional microbial communities to N addition (Avrahami et al., 2002; Li and Gu, 2013). Significant positive correlations were observed between AOB-*amoA* and *nosZ*

chinaXiv:201811.00111v1

abundances, and also between *nirK* and *nosZ* abundances at the short-term site (Fig. 5), indicating a combined gene regulation on $N_2O$ emissions from both nitrification and denitrification pathways (Zhang et al., 2014; Tang et al., 2016; Domeignoz-Horta et al., 2017). However, this close relationship linking both nitrifying and denitrifying functional groups was not found at the long-term site. Possibly because that the short-term N addition induced more significant changes in soil properties but this effect was weakened by the long-term N addition. This could be explained by the more significant correlations between soil properties (pH, C/N ratio, total N and $NH_4^+$-N) and functional gene abundances at the short- than long-term site (Fig. 5). The positive correlation between *nosZ* abundance and $N_2O$ flux observed at the short-term N addition site seems a contradiction, possibly because the $N_2O$ flux we calculated was a sum of three $N_2O$ emission fractions associating autotrophic nitrification, heterotrophic nitrification and denitrification pathways (Zhang et al., 2011). However, at the long-term site, we only found a significant negative correlation between pH and AOB-*amoA* abundance, and a significant positive correlation between AOA-*amoA* abundance and $N_2O$ flux (Fig. 5), implying a relatively looser relationship among soil properties, gene abundance and $N_2O$ fluxes. Previous study suggested that soil properties and microbial community may distinctly play dominant roles in explaining lower and higher $N_2O$ emission rates, respectively (Domeignoz-Horta et al., 2017). This triggers our speculation of possible reasons for the quite different relationships of soil, gene and $N_2O$ between the short- and long-term sites: the deepened acidification in the long-term site soil induced not only the community changes but also the ecological niche distinctions of the two ammonia oxidizers (AOA and AOB) (Nicol et al., 2008; Hu et al., 2013; Remy et al., 2018). Moreover, the change of soil conditions under the long-term N addition also reduced the close relationship between AOA and

chinaXiv:201811.00111v1

other variables in this acid soil (Hu et al., 2013) and finally induced the positive correlation between pH and AOB-*amoA* abundance. Briefly, the changed soil and climatic conditions (rainfall, moisture, temperature, etc.) affected microbial activities and gene abundance related to $N_2O$ production and further reduction to $N_2$ which is affected by soil acidity (Liu et al., 2014). Thus, the relationship among soil properties, gene abundance and $N_2O$ fluxes at the short-term N addition site is much tighter than that at the long-term site where microbial communities have adapted to prevailing conditions.

Our results showed a changed functional gene regulation in the subtropical forest $N_2O$ emission as a response to prolonged N addition duration. However, it is still obscured for the understanding of soil nitrifying and denitrifying functional group changes from only the functional gene abundance aspect since the operating of gene function is reflected by corresponding gene transcripts (Xu et al., 2012; Wu et al., 2017). So for a better elucidating the importance of the internal mechanisms of soil microbial functional groups in regulating $N_2O$ emissions, studies of corresponding RNA transcripts and their relationships with $N_2O$ productions (Liu et al., 2014; Liu et al., 2010; Hassan et al., 2016) are needed to be conducted in the future. Moreover, the comprehensive exploration of soil microbial responses to N depositions from microbial structures, gene abundance and transcription levels need to be done in the future (Li and Gu, 2013).

*4.4 $N_2O$ productions in relation to N additions, N transformations and functional gene regulations*

Consistent with previous results (Zhang et al., 2011), the contribution of



chinaXiv:201811.00111v1

heterotrophic nitrification was lower than denitrification but was higher than autotrophic nitrification to total $N_2O$ fluxes (Fig. 2b). However, the higher heterotrophic than autotrophic nitrification contribution is not reflected by either the significantly higher gross autotrophic nitrification than heterotrophic nitrification rates or by the most abundant AOA-*amoA* (Table S4, Fig. 4b), while the most dominant denitrification contribution is also inconsistent with the relatively less abundant denitrifiers (*nirK* + *nosZ*) than nitrifiers (AOA-*amoA* + AOB-*amoA*) in the forest soil (Fig. 4c). Based on the conceptual "hole-in-the-pipe" (HIP) model of $N_2O$ emission and the modifications of the model (Firestone and Davidson, 1989; Zhang et al., 2014; Zhang et al., 2015), we speculate possible reasons for the inconsistence among functional gene abundance, N transformation rates and $N_2O$ emissions: the more abundant AOA in soil contributed to a higher autotrophic nitrification rate but also triggered a bigger $N_2O$ leaking "hole" from the "pipe" of this pathway. The lower heterotrophic nitrification rate induced a smaller "hole" for $N_2O$ leaking, so a considerable proportion of $N_2O$ production via this pathway maintained. Denitrification plays as an essential pathway for $NO_3^-$ removing from this subtropical forest (Fang et al., 2015), but the higher *nirK* than *nosZ* abundance in the forest soil potentially induces more $N_2O$ production than $N_2O$ reduction, thus finally induced the highest contribution of denitrification to $N_2O$ emission (Fig. 2b).

Our study in the subtropical forest revealed a change of the response patterns in specific N transformation rates to long-term N addition (Fig. 3), further directing a change in the transformation fates of $NH_4^+$ and $NO_3^-$, including the production of $NH_4^+$ via the mineralization of soil labile and recalcitrant organic N and the consumption of $NH_4^+$ via autotrophic nitrification, the production of $NO_3^-$ via autotrophic and heterotrophic nitrifications and the consumption of $NO_3^-$ via

chinaXiv:201811.00111v1

immobilization and DNRA, respectively, to the prolonged N addition. Thus the different responses of net $NO_3^-$ production to increased N addition at the two sites (Fig. 3g) further reflect a change of $NO_3^-$ retention potential in the subtropical forest soil with N addition duration prolong. Our study revealed that soil functional genes, especially the two nitrifying functional genes (AOB-*amoA*, AOA-*amoA*) changed more in responding to prolonged N addition (Fig. 4). However, it is still controversial to conclude that the insignificant change of $N_2O$ under the long-term N addition is a combined response pattern of the four genes that currently studied. The emission rate of $N_2O$ is a reflection balancing the regulations among nitrifying $N_2O$-producers (AOB-*amoA*, AOA-*amoA*), denitrifying $N_2O$-producers (*nirK*/*nirS*) and denitrifying-$N_2O$ reducers (*nosZ*). So the fully understanding of other functional groups that not considered in the present study but are of great importance for $N_2O$ emission, including *nirS* gene for $N_2O$ production from NO, and the newly identified $N_2O$-reducting clade recently for the $N_2O$ reduction to $N_2$, needs to be done in the future (Levy-Booth et al., 2014; Zhang et al., 2014; Tang et al., 2016; Domeignoz-Horta et al., 2017). Correspondingly, NO as an intermediate production and $N_2$ as a final production in both nitrification and denitrification processes cannot be neglected in future studies because of their close linkage with $N_2O$ production and consumption (Zhang et al., 2014; Zhang et al., 2015; Tang et al., 2016).

In this study, we simulated N deposition by adding equal amounts of $NH_4^+$ and $NO_3^-$ ($NH_4NO_3$) to subtropical forest soils. Natural atmospheric N depositions usually show unequal contributions from these two inorganic N forms, with a ratio of approximately 60/40 ($NH_4^+/NO_3^-$) (Fang et al., 2011; Fang et al., 2015). A study of two subtropical masson pine forests in south China even found a ratio of about 70/30 (Chen et al., 2004), thus providing different transformation capacities of deposited

chinaXiv:201811.00111v1

$NH_4^+$ and $NO_3^-$. The studied subtropical forest in DHSBR has received atmospheric N deposition at an amount of more than 30 kg N $ha^{-1}$ $a^{-1}$ since 1990, so the long-term natural N accumulation in the forest soils might be one of the reasons for the significant net $NO_3^-$ production in our findings, although leaching and denitrification have been proved to be main fates of the produced $NO_3^-$ in this forest (Fang et al., 2009; Fang et al., 2015). Although high autotrophic nitrification rates were measured in almost all the N addition treatments at the two sites, we did not find a correspondingly high $^{15}N$ enrichment in $N_2O$. One reason for this result could be high conversion rates of $N_2O$ to $N_2$. So the determination of the $^{15}N$ enrichment in $N_2$ should be considered in future studies. Despite the obvious changes of specific soil N transformation rates and gene abundances but not $N_2O$ fluxes in responding to long-term N addition, we still found a looser relationship among soil properties, functional gene abundance and $N_2O$ fluxes at the long-term site than the short-term site based on correlation analysis results. We argue that functional microbial community adaptations occur which are developing in response to prevailing soil conditions and high natural ambient N depositions. This is in line with the response of microbial community structure, diversity and also gene expression to changing biotic and abiotic factors (Avrahami et al., 2002; Smith et al., 2010; Németh et al., 2014), while the effect of N deposition is a prevailing factor over other influencing factors. This would also explain the change of the correlations between functional gene abundance and $N_2O$ flux with the N addition duration prolong (Fig. 5). However, to elucidate this further microbial activity shifts rather than just focusing on gene expressions would most likely be more indicative.

## 5. Conclusion



chinaXiv:201811.00111v1

In this study, we compared the response of $N_2O$ emissions, N transformations as well as gene regulation traits between two subtropical evergreen broadleaf forest sites that have received either one year (short-term) or 12 years (long-term) of simulated N deposition. Our results revealed that, long-term N addition did not induce significant changes in $N_2O$ fluxes, soil N transformation rates and functional gene abundances. However, compared with the short-term N addition: i) long-term N addition changed the response of specific N transformation rates, especially the rate of N transformation processes that related to the fate of $NH_4^+$ and $NO_3^-$ (mineralization, nitrification, $NO_3^-$ immobilization and the dissimilatory $NO_3^-$ reduction to $NH_4^+$); ii) long-term N addition induced more changes in the response of soil nitrifying $N_2O$-producters (AOA-*amoA*, AOB-*amoA*) to N treatments than that in the response of denitrifying $N_2O$-producers (*nirK*) or $N_2O$-reducers (*nosZ*); iii) long-term N addition weakened the close correlations among soil properties, functional gene abundance and $N_2O$ fluxes that observed at the short-term site. However, the observed differences of N dynamics and $N_2O$ emission traits at the two simulated N deposition sites cannot be solely explained by soil microbial nitrifying and denitrifying functional genes. Soil microenvironment conditions (pH, substrate availability, etc.) and their transition effects from the short-term to long-term N depositions are key to understanding microbial functional gene expressions and gene associated N dynamics (including $N_2O$). We argue that microbial regulation adaptations exist to prevailing soil conditions in response to long-term natural and anthropogenic N depositions.

chinaXiv:201811.00111v1

**Acknowledgments**

This work was financially supported by the National Natural Science Foundation of China (31425005, 31290222, 31400420) and the Guangdong Province Baiqianwan Talents Program. We thank Dinghushan Forest Ecosystem Research Station, CAS for platform support; Jiangming Mo and Xiankai Lu for their approval of sample collections at the long-term site; and Jinhong He, Wenjuan Wang and Yanxia Nie for their help with laboratory assays. We sincerely thank the two anonymous reviewers who provided constructive comments for improving this paper. This study was carried out as an associated project to the German Science foundation research unit DASIM "Denitrification in Agricultural Soils: Integrated control and Modelling at various scales" (FOR2337).

chinaXiv:201811.00111v1

**References**

Alm, J., Shurpali, N.J., Minkkinen, K., Aro, L., Hytonen, J., Laurila, T., Lohila, A., Maljanen, M., Martikainen, P.J., Makiranta, P., Penttila, T., Saarnio, S., Silvan, N., Tuittila, E.S., Laine, J., 2007. Emission factors and their uncertainty for the exchange of $CO_2$, $CH_4$ and $N_2O$ in finnish managed peatlands. Boreal Environ. Res. 12, 191-209.

Avrahami, S., Conrad, R., Braker, G., 2002. Effect of soil ammonium concentration on $N_2O$ release and on the community structure of ammonia oxidizers and denitrifiers. Appl. Environ. Micro. 68, 5685-5692.

Bai, E., Li, W., Li, S.L., Sun, J.F., Peng, B., Dai, W.W., Jiang, P., Han, S.J., 2014. Pulse increase of soil $N_2O$ emission in response to N addition in a temperate forest on Mt Changbai, Northeast China. Plos One 9, e102765, doi: 10.1371/journal.pone.0102765.

Bárta, J., Melichová, T., Vaněk, D., Picek, T., Šantrůčková, H., 2010. Effect of pH and

dissolved organic matter on the abundance of *nirK* and *nirS* denitrifiers in spruce forest soil. Biogeochemistry 101, 123-132.

Bengtsson, G., Bengtson, P., Mansson, K.F., 2003. Gross nitrogen mineralization-, immobilization-, and nitrification rates as a function of soil C/N ratio and microbial activity. Soil Biol. Biochem. 35, 143-154.

Boy, J., Rollenbeck, R., Valarezo, C., Wilcke, W., 2008. Amazonian biomass burning-derived acid and nutrient deposition in the north Andean montane forest of Ecuador. Global Biogeochem. Cy. 22, GB4011, doi:10.1029/2007GB003158.

Braker, G., Conrad, R., 2011. Diversity, structure, and size of $N_2O$-producing microbial communities in soils—what matters for their functioning? Advances in Applied Microbiology. Academic Press, Burlington, pp. 33-70.

Bremner, J.M., 1997. Sources of nitrous oxide in soils. Nutr. Cycl. Agroecosys. 49, 7-16.

Breuer, L., Papen, H., Butterbach-Bahl, K., 2000. N2O emission from tropical forest soils of Australia. J. Geophys. Res-Atmos. 105, 26353-26367.

Butterbach-Bahl, K., Baggs, E.M., Dannenmann, M., Kiese, R., Zechmeister-Boltenstern, S., 2013. Nitrous oxide emissions from soils: how well do we understand the processes and their controls? Philos. T. R. Soc. B. Sciences 368, doi: 10.1098/rstb.2013.0122.

Chatskikh, D., Olesen, J.E., Berntsen, J., Regina, K., Yamulki, S., 2005. Simulation of effects of soils, climate and management on $N_2O$ emission from grasslands. Biogeochemistry 76, 395-419.

Chen, C., Chen, D.L., Pan, J.J., Lam, S.K., 2014. Analysis of factors controlling soil $N_2O$ emission by principal component and path analysis method. Environ. Earth Sci. 72, 1511-1517.



chinaXiv:201811.00111v1

Chen, J., Xiao, G.L., Kuzyakov, Y., Jenerette, G.D., Ma, Y., Liu, W., Wang, Z.F., Shen, W.J., 2017. Soil nitrogen transformation responses to seasonal precipitation changes are regulated by changes in functional microbial abundance in a subtropical forest. Biogeosciences 14, 2513-2525.

Chen, Q.Q., Shen, C.D., Sun, Y.M., Peng, S.L., Yi, W.X., Li, Z.A., Jiang, M.T., 2005. Spatial and temporal distribution of carbon isotopes in soil organic matter at the Dinghushan Biosphere Reserve, South China. Plant Soil 273, 115-128.

Chen, X.Y., Mulder, J., Wang, Y.H., Zhao, D.W., Xiang, R.J., 2004. Atmospheric deposition, mineralization and leaching of nitrogen in subtropical forested catchments, South China. Environ. Geochem. Hlth. 26, 179-186.

Chen, Y., Randerson, J.T., Van Der Werf, G.R., Morton, D.C., Mu, M., Kasibhatla, P.S., 2010. Nitrogen deposition in tropical forests from savanna and deforestation fires. . Global Change Biol. 16, 2024-2038.

Cheng, Y., Wang, J., Wang, S.Q., Zhang, J.B., Cai, Z.C., 2014. Effects of soil moisture on gross N transformations and $N_2O$ emission in acid subtropical forest soils. Biol. Fert. Soils 50, 1099-1108.

Corre, M.D., Sueta, J.P., Veldkamp, E., 2014. Nitrogen-oxide emissions from tropical forest soils exposed to elevated nitrogen input strongly interact with rainfall quantity and seasonality. Biogeochemistry 118, 103-120.

Cui, P.Y., Fan, F.L., Yin, C., Song, A., Huang, P.R., Tang, Y.J., Zhu, P., Peng, C., Li, T.Q., Wakelin, S.A., Liang, Y.C., 2016. Long-term organic and inorganic fertilization alters temperature sensitivity of potential $N_2O$ emissions and associated microbes. Soil Biol. Biochem. 93, 131-141.

Cusack, D.F., Silver, W.L., Torn, M.S., Burton, S.D., Firestone, M.K., 2011. Changes in microbial community characteristics and soil organic matter with nitrogen

chinaXiv:201811.00111v1

additions in two tropical forests. Ecology 92, 621-632.

Deppe, M., Well, R., Giesemann, A., Spott, O., Flessa, H., 2017. Soil $N_2O$ fluxes and related processes in laboratory incubations simulating ammonium fertilizer depots. Soil Biol. Biochem. 104, 68-80.

Domeignoz-Horta, L.A., Philippot, L., Peyrard, C., Bru, D., Breuil, M.C., Bizouard, F., Justes, E., Mary, B., Leonard, J., Spor, A., 2017. Peaks of in situ $N_2O$ emissions are influenced by $N_2O$-producing and reducing microbial communities across arable soils. Glob Chang Biol. 1-11. doi: 10.1111/gcb.13853

Domeignoz-Horta, L.A., Spor, A., Bru, D., Breuil, M.C., Bizouard, F., Leonard, J., Philippot, L., 2015. The diversity of the $N_2O$ reducers matters for the $N_2O$:$N_2$ denitrification end-product ratio across an annual and a perennial cropping system. Front. Microbiol. 6, 971.

Du, E.Z., Jiang, Y., Fang, J.Y., de Vries, W., 2014. Inorganic nitrogen deposition in China's forests: Status and characteristics. Atmos. Environ. 98, 474-482.

Faeflen, J.S., Li, S.W., Xin, X.P., Wright, A.L., Jiang, X.J., 2016. Autotrophic and heterotrophic nitrification in a highly acidic subtropical pine forest soil. Pedosphere 26, 904-910.

Fang, Y.T., Gundersen, P., Zhang, W., Zhou, G.Y., Christiansen, J.R., Mo, J.M., Dong, S.F., Zhang, T., 2008a. Soil–atmosphere exchange of $N_2O$, $CO_2$ and $CH_4$ along a slope of an evergreen broad-leaved forest in southern China. Plant Soil 319, 37-48.

Fang, Y.T., Gundersen, P., Mo, J.M., Zhu, W.X., 2008b. Input and output of dissolved organic and inorganic nitrogen in subtropical forests of South China under high air pollution. Biogeosciences 5, 339-352.

Fang, Y.T., Gundersen, P., Mo, J.M., Zhu, W.X., 2009. Nitrogen leaching in response to



chinaXiv:201811.00111v1

increased nitrogen inputs in subtropical monsoon forests in southern China. Forest Ecol. Manag. 257, 332-342.

Fang, Y.T., Gundersen, P., Vogt, R.D., Koba, K., Chen, F.S., Chen, X.Y., Yoh, M., 2011. Atmospheric deposition and leaching of nitrogen in Chinese forest ecosystems. J. Forest Res. 16, 341-350.

Fang, Y.T., Koba, K., Makabe, A., Takahashi, C., Zhu, W.X., Hayashi, T., Hokari, A.A., Urakawa, R., Bai, E., Houlton, B.Z., Xia, D., Zhang, S.S., Matsushita, K., Tu, Y., Liu, D.W., Zhu, F.F., Wang, Z.Y., Zhou, G.Y., Chen, D.X., Makita, T., Toda, H., Liu, X.Y., Chen, Q.S., Zhang, D.Q., Li, Y.D., Yoh, M., 2015. Microbial denitrification dominates nitrate losses from forest ecosystems. P. Natl. Acad. Sci. USA 112, 1470-1474.

FAO., 1998. World Reference Base for Soil Resources. Vol 84. Rome, Italy.

Feast, N.A., Dennis, P.F., 1996. A comparison of methods for nitrogen isotope analysis of groundwater. Chem. Geol. 129, 167-171.

Firestone, M.K., Davidson, E.A., 1989. Microbiological basis of NO and $N_2O$ production and consumption in soil. In: Andreae, M.O., Schimel, D.S. (Eds.), Exchange of trace gases between terrestrial ecosystems and the atmosphere. John Wiley & Sons, New York.

Freedman, Z., Eisenlord, S.D., Zak, D.R., Xue, K., He, Z., Zhou, J., 2013. Towards a molecular understanding of N cycling in northern hardwood forests under future rates of N deposition. Soil Biol. Biochem. 66, 130-138.

Frey, S.D., Knorr, M., Parrent, J.L., Simpson, R.T., 2004. Chronic nitrogen enrichment affects the structure and function of the soil microbial community in temperate hardwood and pine forests. Forest Ecol. Manag. 196, 159-171.

Galloway, J.N., Dentener, F.J., Capone, D.G., Boyer, E.W., Howarth, R.W., Seitzinger,

chinaXiv:201811.00111v1

S.P., Asner, G.P., Cleveland, C.C., Green, P.A., Holland, E.A., Karl, D.M., Michaels, A.F., Porter, J.H., Townsend, A.R., Vorosmarty, C.J., 2004. Nitrogen cycles: past, present, and future. Biogeochemistry 70, 153-226.

Galloway, J.N., Townsend, A.R., Erisman, J.W., Bekunda, M., Cai, Z.C., Freney, J.R., Martinelli, L.A., Seitzinger, S.P., Sutton, M.A., 2008. Transformation of the nitrogen cycle: Recent trends, questions, and potential solutions. Science 320, 889-892.

Gao, W.L., Kou, L., Zhang, J.B., Muller, C., Wang, H.M., Yang, H., Li, S.G., 2016. Enhanced deposition of nitrate alters microbial cycling of N in a subtropical forest soil. Biol. Fert. Soil 52, 977-986.

Gao, W.L., Yang, H., Kou, L., Li, S.G., 2015. Effects of nitrogen deposition and fertilization on N transformations in forest soils: a review. J. Soil. Sediment. 15, 863-879.

Gubry-Rangin, C., Nicol, G.W., Prosser, J.I., 2010. Archaea rather than bacteria control nitrification in two agricultural acidic soils. FEMS Microbiol. Ecol. 74, 566-574.

Gurmesa, G.A., Lu, X.K., Gundersen, P., Mao, Q.G., Zhou, K.J., Fang, Y.T., Mo, J.M., 2016. High retention of 15 N-labeled nitrogen deposition in a nitrogen saturated old-growth tropical forest. Global Change Biol. 22, 3608-3620.

Hallin, S., Philippot, L., Löffler, F., Sanford, R.A., Jones, C.M., 2017. Genomics and ecology of novel $N_2O$ reducing microorganisms. Trends Microbiol. Online first.

Hart, S.C., Nason, G.E., Myrold, D.D., Perry, D.A., 1994. Dynamics of gross nitrogen transformations in an old-growth forest - the carbon connection. Ecology 75, 880-891.

Hassan, J., Qu, Z., Bergaust, L.L., Bakken, L.R., 2016. Transient accumulation of $NO_2^-$ and $N_2O$ during denitrification explained by assuming cell diversification by

chinaXiv:201811.00111v1

stochastic transcription of denitrification genes. Plos Comput. Biol. 12, e1004621.

Herrmann, M., Pust, J., Pott, R., 2005. Leaching of nitrate and ammonium in heathland and forest ecosystems in Northwest Germany under the influence of enhanced nitrogen deposition. Plant Soil 273, 129-137.

Hu, H.W., Zhang, L.M., Dai, Y., Di, H.J., He, J.Z., 2013. pH-dependent distribution of soil ammonia oxidizers across a large geographical scale as revealed by high-throughput pyrosequencing. J. Soil Sediment. 13, 1439-1449.

Isobe, K., K., K., Suwa, Y., Ikutani, J., Fang, Y.T., Yoh, M., Mo, J.M., Otsuka, S., Senoo, K., 2012. High abundance of ammonia-oxidizing archaea in acidified subtropical forest soils in southern China after long-term N deposition. FEMS Microbiol. Ecol. 80, 193-203.

Janssens, I.A., Dieleman, W., Luyssaert, S., Subke, J.A., Reichstein, M., Ceulemans, R., Ciais, P., Dolman, A.J., Grace, J., Matteucci, G., Papale, D., Piao, S.L., Schulze, E.D., Tang, J., Law, B.E., 2010. Reduction of forest soil respiration in response to nitrogen deposition. Nat. Geosci. 3, 315-322.

Jones, C.M., Graf, D.R.H., Bru, D., Philippot, L., Hallin, S., 2013. The unaccounted yet abundant nitrous oxide-reducing microbial community: a potential nitrous oxide sink. Isme J. 7, 417-426.

Kanakidou, M., Myriokefalitakis, S., Daskalakis, N., Fanourgakis, G., Nenes, A., Baker, A.R., Tsigaridis, K., Mihalopoulos, N., 2016. Past, present, and future atmospheric Nitrogen deposition. J. Atmos. Sci. 73, 2039-2047.

Kiese, R., Hewett, B., Graham, A., Butterbach-Bahl, K., 2003. Seasonal variability of $N_2O$ emissions and $CH_4$ uptake by tropical rainforest soils of Queensland, Australia. Global Biogeochem. Cy. 17, 2002GB002014.

Koranda, M., Kaiser, C., Fuchslueger, L., Kitzler, B., Sessitsch, A., Zechmeister-



chinaXiv:201811.00111v1

Boltenstern, S., Richter, A., 2014. Fungal and bacterial utilization of organic substrates depends on substrate complexity and N availability. FEMS Microbiol. Ecol. 87, 142-152.

Levy-Booth, D.J., Prescott, C.E., Grayston, S.J., 2014. Microbial functional genes involved in nitrogen fixation, nitrification and denitrification in forest ecosystems. Soil Biol. Biochem. 75, 11-25.

Li, M., Gu, J.D., 2013. Community structure and transcript responses of anammox bacteria, AOA, and AOB in mangrove sediment microcosms amended with ammonium and nitrite. Appl. Microbiol. Biot. 97, 9859-9874.

Liu, B., Frostegard, A., Bakken, L.R., 2014. Impaired reduction of $N_2O$ to $N_2$ in acid soils is due to a posttran scriptional interference with the expression of *nosZ*. mBio 5, doi: 10.1128/mBio.01383-14.

Liu, B.B., Mørkved, P.T., Frostegård, Å., Bakken, L.R., 2010. Denitrification gene pools, transcription and kinetics of NO, $N_2O$ and $N_2$ production as affected by soil pH. FEMS Microbiol. Ecol. 72, 407-417.

Liu, G.S., 1996. Soil physical and chemical analysis and description of soil profiles. Chinese standars press, Beijing (in Chinese).

Liu, X.J., Duan, L., Mo, J.M., Du, E.Z., Shen, J.L., Lu, X.K., Zhang, Y., Zhou, X.B., He, C.E., Zhang, F.S., 2011. Nitrogen deposition and its ecological impact in China: An overview. Environ. Pollut. 159, 2251-2264.

Long, X.E., Chen, C.R., Xu, Z.H., Oren, R., He, J.Z., 2012. Abundance and community structure of ammonia-oxidizing bacteria and archaea in a temperate forest ecosystem under ten-years elevated $CO_2$. Soil Biol. Biochem. 46, 163-171.

Lu, X., Gilliam, F.S., Yu, G., Li, L., Mao, Q., Chen, H., Mo, J., 2013. Long-term nitrogen addition decreases carbon leaching in a nitrogen-rich forest ecosystem.



chinaXiv:201811.00111v1

Biogeosciences 10, 3931-3941.

Lu, X.K., Mo, J.M., Dong, F.S., 2008. Effects of nitrogen deposition on forest biodiversity. Acta Ecologica Sinica 28, 5532-5548.

Maaroufi, N.I., Nordin, A., Hasselquist, N.J., Bach, L.H., Palmqvist, K., Gundale, M.J., 2015. Anthropogenic nitrogen deposition enhances carbon sequestration in boreal soils. Global Change Biol. 21, 3169-3180.

MacDonald, J.A., Dise, N.B., Matzner, E., Armbruster, M., Gundersen, P., Forsius, M., 2002. Nitrogen input together with ecosystem nitrogen enrichment predict nitrate leaching from European forests. Global Change Biol. 8, 1028-1033.

Matson, P., Lohse, K.A., Hall, S.J., 2002. The globalization of nitrogen deposition: Consequences for terrestrial ecosystems. Ambio 31, 113-119.

Mo, J.M., Brown, S., Xue, J.H., Fang, Y.T., Li, Z.A., 2006. Response of litter decomposition to simulated N deposition in disturbed, rehabilitated and mature forests in Subtropical China. Plant Soil 282, 135-151.

Müller, C., Laughlin, R.J., Spott, O., Rütting, T., 2014. Quantification of $N_2O$ emission pathways via a $^{15}N$ tracing model. Soil Biol. Biochem. 72, 44-54.

Müller, C., Rütting, T., Kattge, J., Laughlin, R.J., Stevens, R.J., 2007. Estimation of parameters in complex 15N tracing models by Monte Carlo sampling. Soil Biol. Biochem. 39, 715-726.

Müller, C., Sherlock, R.R., Williams, P.H., 1998. Field method to determine $N_2O$ emission from nitrification and denitrification. Biol. Fert. Soils 28, 51-55.

Németh, D.D., Wagner-Riddle, C., Dunfield, K.E., 2014. Abundance and gene expression in nitrifier and denitrifier communities associated with a field scale spring thaw $N_2O$ flux event. Soil Biol. Biochem. 73, 1-9.

Nicol, G.W., Leininger, S., Schleper, C., Prosser, J.I., 2008. The influence of soil pH on

chinaXiv:201811.00111v1

the diversity, abundance and transcriptional activity of ammonia oxidizing archaea and bacteria. Environ. Microbiol. 10, 2966-2978.

Orellana, L.H., Rodriguez-R, L.M., Higgins, S., Chee-Sanford, J.C., Sanford, R.A., Ritalahti, K.M., Loffler, F.E., Konstantinidis, K.T., 2014. Detecting nitrous oxide reductase (*nosZ*) genes in soil metagenomes: Method development and implications for the nitrogen cycle. mBio 5, 3, doi: 10.1128/mBio.01193-14.

Prieme, A., Braker, G., Tiedje, J.M., 2002. Diversity of nitrite reductase (*nirK* and *nirS*) gene fragments in forested upland and wetland soils. Appl. Environ.Microb. 68, 1893-1900.

Qafoku, N.P., Van Ranst, E., Noble, A., Baert, G., 2004. Variable charge soils: Their mineralogy, chemistry and management. Adv. Agron. 84, 159-215.

Remy, E., Wuyts, K., Verheyen, K., Gundersen, P., Boeckx, P., 2018. Altered microbial communities and nitrogen availability in temperate forest edges. Soil Biol. Biochem. 116, 179-188.

Rich, J.J., Heichen, R.S., Bottomley, P.J., Cromack, K., Myrold, D.D., 2003. Community composition and functioning of denitrifying bacteria from adjacent meadow and forest soils. Appl. Environ. Microb. 69, 5974-5982.

Rütting, T., Clough, T.J., Müller, C., Lieffering, M., Newton, P.C.D., 2010. Ten years of elevated atmospheric carbon dioxide alters soil nitrogen transformations in a sheep-grazed pasture. Global Change Biol. 16, 2530-2542.

Schimel, J.P., Bennett, J., 2004. Nitrogen mineralization: Challenges of a changing paradigm. Ecology 85, 591-602.

Sinsabaugh, R.L., Gallo, M.E., Lauber, C., Waldrop, M.P., Zak, D.R., 2005. Extracellular enzyme activities and soil organic matter dynamics for northern hardwood forests receiving simulated nitrogen deposition. Biogeochemistry 75,

chinaXiv:201811.00111v1

201-215.

Smith, J., Wagner-Riddle, C., Dunfield, K., 2010. Season and management related changes in the diversity of nitrifying and denitrifying bacteria over winter and spring. Appl. Soil Ecol. 44, 138-146.

Szukics, U., Abell, G.C.J., Hödl, V., Mitter, B., Sessitsch, A., Hackl, E., Zechmeister-Boltenstern, S., 2010. Nitrifiers and denitrifiers respond rapidly to changed moisture and increasing temperature in a pristine forest soil. FEMS Microbiol. Ecol. 72, 395-406.

Tang, X.L., Liu, S.G., Zhou, G.Y., Zhang, D.Q., Zhou, C.Y., 2006. Soil-atmospheric exchange of $CO_2$, $CH_4$, and $N_2O$ in three subtropical forest ecosystems in southern China. Global Change Biol. 12, 546-560.

Tang, Y.Q., Zhang, X.Y., Li, D.D., Wang, H.M., Chen, F.S., Fu, X.L., Fang, X.M., Sun, X.M., Yu, G.R., 2016. Impacts of nitrogen and phosphorus additions on the abundance and community structure of ammonia oxidizers and denitrifying bacteria in Chinese fir plantations. Soil Biol. Biochem. 103, 284-293.

Vance, E.D., Brookes, P.C., Jenkinson, D.S., 1987. An extraction method for measuring soil microbial biomass-C. Soil Biol. Biochem. 19, 703-707.

Verhamme, D.T., Prosser, J.I., Nicol, G.W., 2011. Ammonia concentration determines differential growth of ammonia-oxidising archaea and bacteria in soil microcosms. Isme J. 5, 1067-1071.

Vet, R., Artz, R.S., Carou, S., Shaw, M., Ro, C.-U., Aas, W., Baker, A., Bowersox, V.C., Dentener, F., Galy-Lacaux, C., Hou, A., Pienaar, J.J., Gillett, R., Forti, M.C., Gromov, S., Hara, H., Khodzher, T., Mahowald, N.M., Nickovic, S., Rao, P.S.P., Reid, N.W., 2014. A global assessment of precipitation chemistry and deposition of sulfur, nitrogen, sea salt, base cations, organic acids, acidity and pH, and



chinaXiv:201811.00111v1

phosphorus. Atmos. Environ. 93, 3-100.

Wang, F.M., Li, J., Wang, X.L., Zhang, W., Zou, B., Neher, D.A., Li, Z.A., 2014a. Nitrogen and phosphorus addition impact soil $N_2O$ emission in a secondary tropical forest of South China. Scientific Rep-UK 4, doi: 10.1038/srep05615.

Wang, J., Zhu, B., Zhang, J.B., Muller, C., Cai, Z.C., 2015. Mechanisms of soil N dynamics following long-term application of organic fertilizers to subtropical rain-fed purple soil in China. Soil Biol. Biochem. 91, 222-231.

Wang, Y.S., Cheng, S.L., Fang, H.J., Yu, G.R., Xu, M.J., Dang, X.S., Li, L.S., Wang, L., 2014b. Simulated nitrogen deposition reduces $CH_4$ uptake and increases $N_2O$ emission from a subtropical plantation forest soil in Southern China. Plos One 9.

Werner, C., Kiese, R., Butterbach-Bahl, K., 2007. Soil-atmosphere exchange of $N_2O$, $CH_4$, and $CO_2$ and controlling environmental factors for tropical rain forest sites in western Kenya. J. Geophys. Res-Atmos. 112, doi: 10.1029/2006JD007388.

Wertz, S., Leigh, A.K.K., Grayston, S.J., 2012. Effects of long-term fertilization of forest soils on potential nitrification and on the abundance and community structure of ammonia oxidizers and nitrite oxidizers. FEMS Microbiol. Ecol. 79, 142-154.

Williams, E.J., Hutchinson, G.L., Fehsenfeld, F.C., 1992. $NO_x$ and $N_2O$ emissions from soil. Global Biogeochem. Cy. 6, 351-388.

Wu, R.N., Meng, H., Wang, Y.F., Lan, W.S., Gu, J.D., 2017. A more comprehensive community of Ammonia-Oxidizing Archaea (AOA) revealed by genomic DNA and RNA analyses of *amoA* gene in subtropical acidic forest soils. Microbial Ecol. 74, 910-922.

Xie, Y., Zhang, J.B., Meng, L., Müller, C., Cai, Z.C., 2015. Variations of soil N transformation and $N_2O$ emissions in tropical secondary forests along an aridity



chinaXiv:201811.00111v1

gradient. J. Soil Sediment 15, 1538-1548.

Xu, Y.B., Cai, Z.C., 2007. Denitrification characteristics of subtropical soils in China affected by soil parent material and land use. Eur. J. Soil Sci. 58, 1293-1303.

Xu, Y.B., Cai, Z.C., Xu, Z.H., 2012. Production and consumption of N2O during denitrification in subtropical soils of China. J. Soil Sediment 12, 1339-1349.

Yu, Y.J., Zhang, J.B., Chen, W.W., Zhong, W.H., Zhu, T.B., Cai, Z.C., 2014. Effect of land use on the denitrification, abundance of denitrifiers, and total nitrogen gas production in the subtropical region of China. Biol. Fert. Soils 50, 105-113.

Zhang, J.B., Müller, C., Cai, Z.C., 2015. Heterotrophic nitrification of organic N and its contribution to nitrous oxide emissions in soils. Soil Biol. Biochem. 84, 199-209.

Zhang, J.B, Yu, Y.J., Zhu, T.B., Cai, Z.C., 2014. The mechanisms governing low denitrification capacity and high nitrogen oxide gas emissions in subtropical forest soils in China. J. Geophys. Res-Biogeo. 119, 1670-1683.

Zhang, J.B., Cai, Z.C., Zhu, T.B., 2011. $N_2O$ production pathways in the subtropical acid forest soils in China. Environ. Res. 111, 643-649.

Zhang, L.M., Hu, H.W., Shen, J.P., He, J.Z., 2012. Ammonia-oxidizing archaea have more important role than ammonia-oxidizing bacteria in ammonia oxidation of strongly acidic soils. Isme J. 6, 1032-1045.

Zhang, W., Mo, J.M., Yu, G.R., Fang, Y.T., Li, D.J., Lu, X.K., Wang, H., 2008. Emissions of nitrous oxide from three tropical forests in Southern China in response to simulated nitrogen deposition. Plant Soil 306, 221-236.

Zhong, Y.Q.W., Yan, W.M., Shangguan, Z.P., 2015. Impact of long-term N additions upon coupling between soil microbial community structure and activity, and nutrient-use efficiencies. Soil Biol. Biochem. 91, 151-159.

chinaXiv:201811.00111v1

Zhu, J., Mulder, J., Wu, L.P., Meng, X.X., Wang, Y.H., Dörsch, P., 2013a. Spatial and temporal variability of $N_2O$ emissions in a subtropical forest catchment in China. Biogeosciences 10, 1309-1321.

Zhu, J.X., He, N.P., Wang, Q.F., Yuan, G.F., Wen, D., Yu, G.R., Jia, Y.L., 2015. The composition, spatial patterns, and influencing factors of atmospheric wet nitrogen deposition in Chinese terrestrial ecosystems. Sci. Total Environ. 511, 777-785.

Zhu, T.B., Meng, T.Z., Zhang, J.B., Yin, Y.F., Cai, Z.C., Yang, W.Y., Zhong, W.H., 2013b. Nitrogen mineralization, immobilization turnover, heterotrophic nitrification, and microbial groups in acid forest soils of subtropical China. Biol. Fert. Soils 49, 323-331.

**Figure legends**

**Fig. 1.** The $^{15}N$ enrichment in $N_2O$ during the paired $^{15}N$ tracing incubation (a, c), and $^{15}N_2O/^{15}NH_4^+$ ratios in the ammonium-labelled incubation (b) and $^{15}N_2O/^{15}NO_3^-$ ratios in the nitrate-labelled incubation (d). Symbols (points and lines) in light green and orange denote the short-term N addition treatments and long-term N addition treatments, respectively. SC, SL, SM and SH denote control, low-N, medium-N and high-N treatments at the short-term N addition site, respectively. LC, LL, LM and LH denote control, low-N, medium-N and high-N treatments at the long-term N addition site, respectively. *, **, ***: the difference between $^{15}NH_4^+$-labelled treatment and $^{15}NO_3^-$-labelled treatment is significant at $p < 0.05$, $p < 0.01$ and $p < 0.001$ level, respectively.

**Fig. 2.** Soil $N_2O$ average fluxes (a), specific pathway fractions of emitted $N_2O$ in each N treatment (b) and average pathway contributions over the 14 day incubation of the



chinaXiv:201811.00111v1

subtropical forest soils (c). SC, SL, SM and SH denote control, low-N, medium-N and high-N treatments at the short-term N addition site, respectively. LC, LL, LM and LH denote control, low-N, medium-N and high-N treatments at the long-term N addition site, respectively. The sign "*" above the light green bars in panel a denotes the difference between the corresponding N treatment and other N treatments is significant ($p < 0.05$). Bars in light green, moderate green and dark green in panel b denote the contribution of $N_2O$ fraction that originate from heterotrophic nitrification (h), autotrophic nitrification (a) and denitrification (d), respectively. Areas in light gray, moderate gray and dark gray in panel c denote that during the incubation, the contribution of $N_2O$ fraction that originate from heterotrophic nitrification ($N_2O_h$), autotrophic nitrification ($N_2O_a$) and denitrification ($N_2O_d$), respectively.

**Fig. 3.** The $^{15}N$ tracing model (Müller et al., 2007) and relative change percentages of soil gross/net N transformation rates in the N addition treatments in comparison to controls at the two sites (inset a-g). White squares and black arrows indicate soil N pools and N transformation processes in the tracing model, respectively. $\mathbf{NH_4^+}$: ammonium; $\mathbf{NH_4^+_{ads}}$ : adsorbed $NH_4^+$; $\mathbf{N_{lab}}$: labile organic N; $\mathbf{NO_3^-}$: nitrate; $\mathbf{N_{rec}}$: recalcitrant organic N. $\boldsymbol{M_{Nrec}}$: mineralization of recalcitrant organic nitrogen to $NH_4^+$; $\boldsymbol{I_{NH4\text{-}Nrec}}$: immobilization of $NH_4^+$ to recalcitrant organic nitrogen; $\boldsymbol{M_{Nlab}}$: mineralization of labile organic nitrogen; $\boldsymbol{I_{NH4\text{-}Nlab}}$: immobilization of $NH_4^+$ to labile organic nitrogen; $\boldsymbol{O_{Nrec}}$: oxidation of recalcitrant organic nitrogen to $NO_3^-$; $\boldsymbol{I_{NO3}}$: immobilization of $NO_3^-$ to recalcitrant organic N; $\boldsymbol{O_{NH4}}$: oxidation of $NH_4^+$ to $NO_3^-$ ; $\boldsymbol{D_{NO3}}$: dissimilatory $NO_3^-$ reduction to $NH_4^+$; $\boldsymbol{A_{NH4}}$: adsorption of $NH_4^+$ on cation exchange sites; $\boldsymbol{R_{NH4a}}$: release of $NH_4^+$ on cation exchange sites; $\boldsymbol{NET_{NO3aprod}}$: net $NO_3^-$ production. Insets numbered with a, b, c, d, e, f and g denote the relative change



chinaXiv:201811.00111v1

percentage of $M_{Nlab}$, $M_{Nrec}$, $O_{NH4}$, $D_{NO3}$, $O_{Nrec}$, $I_{NO3}$, and $NET_{NO3aprod}$, respectively. Within each inset, bars in light green and orange denote the results at the short- and long-term sites, respectively. L, M and H in the x-axis denote the low-N, medium-N and high-N treatment, respectively. Numbers in the y-axis denote the relative change percentage (%) of individual N transformation rate in the N addition treatment in comparison to control.

**Fig. 4.** Abundance (copy numbers $g^{-1}$ dry soil) and abundance ratios of the functional genes (AOB-*amoA*, AOA-*amoA*, *nirK* and *nosZ*) under different N treatments at the two sites. Bars in light green and orange denote short-term N addition treatments and long-term N addition treatments, respectively. Inset denote relative change percentage of gene abundance or abundance ratio in N-addition treatments in comparison to control. L, M and H in the x-axis denote the low-N, medium-N and high-N treatment, respectively. Numbers in the y-axis denote the relative change percentage (%) of gene abundance or abundance ratio in N addition treatments in comparison to control. *D* and *N* indicate results of two-way ANOVA analysis: *D* indicates the difference significance between N addition durations (short-term and long-term), and *N* (N level) indicates the difference significance among N treatments. Only significant differences were showed in this figure while insignificant differences were not shown.

**Fig. 5.** Pearson correlation analysis results of soil properties, gene abundances and $N_2O$ fluxes at the short-term and long-term sites. $N_2O$ production pathways that considered in this study, i.e. heterotrophic nitrification, autotrophic nitrification and denitrification, and the roles of the studied functional genes (AOA-*amoA*, AOB-*amoA*, *nirK*, *nosZ*) in regulating $N_2O$ emissions are also shown. White squares and



chinaXiv:201811.00111v1

white ellipses denote N pools and gaseous N forms, respectively. Black arrows denote N transformation directions. The cloud ellipse denotes $N_2O$ fluxes. Green ellipses denote functional genes that are associated with N transformation processes, while the size of the ellipses denote the abundance magnitude of four functional genes found in this study (i.e. larger ellipse indicates higher gene abundance). Dark-yellow squares denote soil properties that are significantly correlated with gene abundances. Light-green lines and orange lines denote significant correlations at the short- and the long-term sites, respectively. The '-' sign in the white ellipse indicates negative correlation. Insignificant correlations were not shown in this figure.

chinaXiv:201811.00111v1

**Fig. 1**

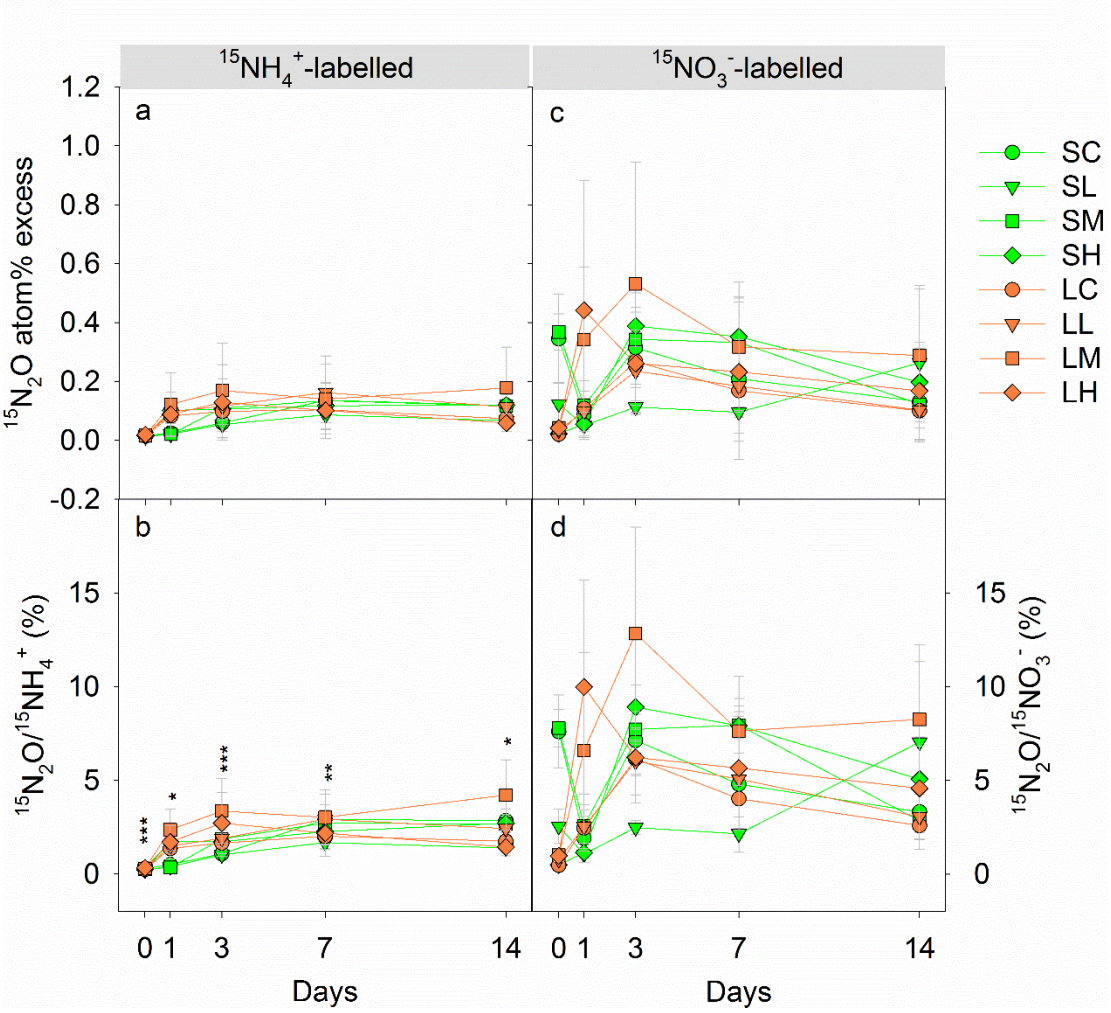


chinaXiv:201811.00111v1

**Fig. 2**

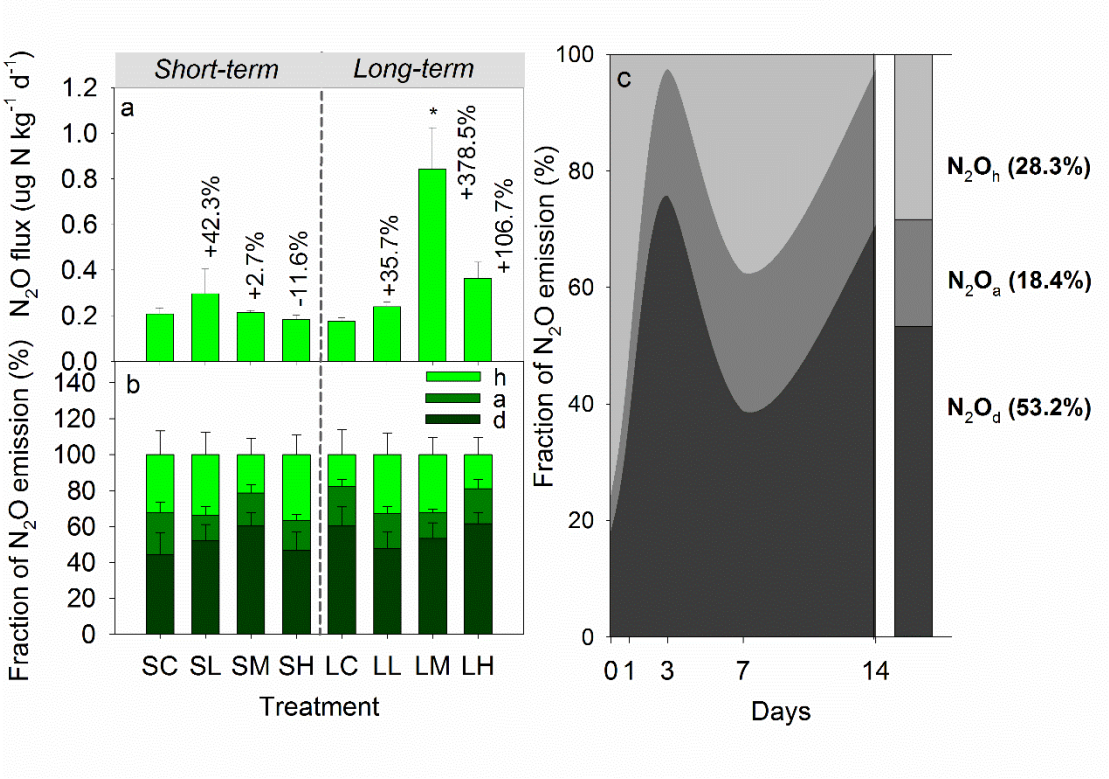


chinaXiv:201811.00111v1

**Fig. 3**

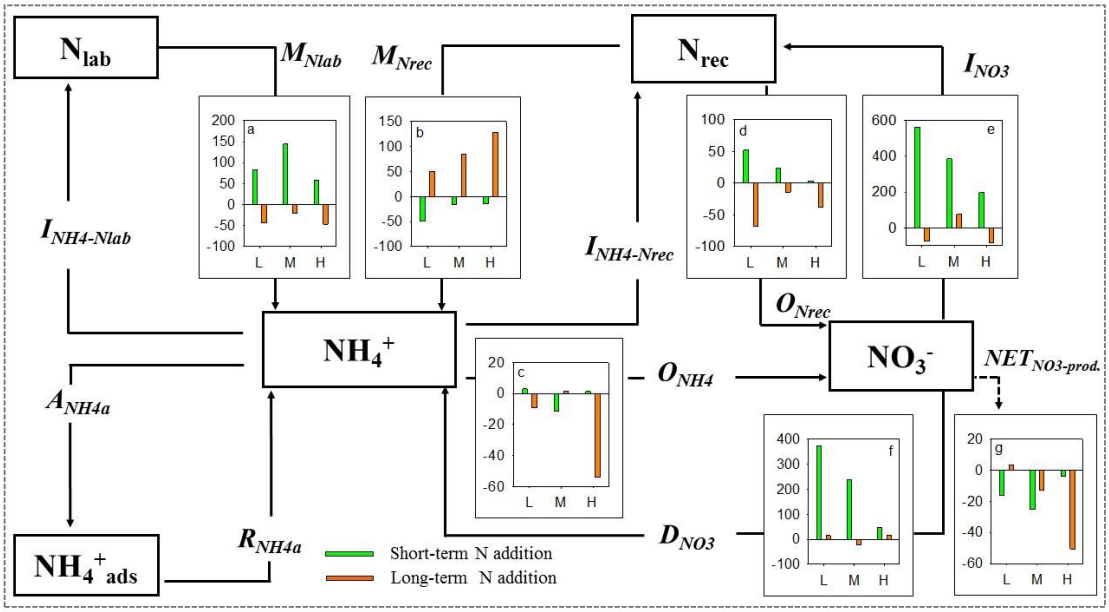


chinaXiv:201811.00111v1

**Fig. 4**

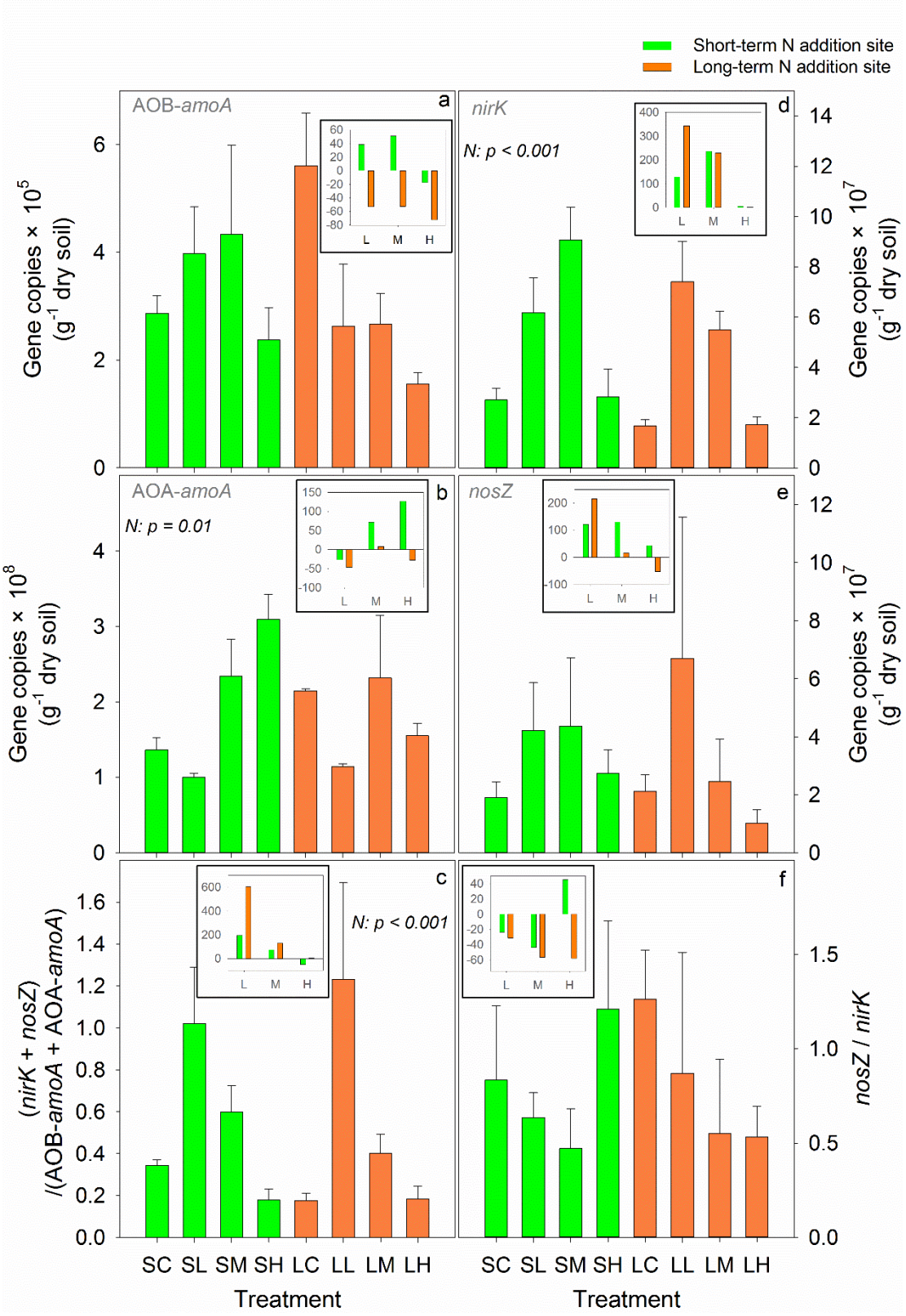


chinaXiv:201811.00111v1

**Fig. 5**

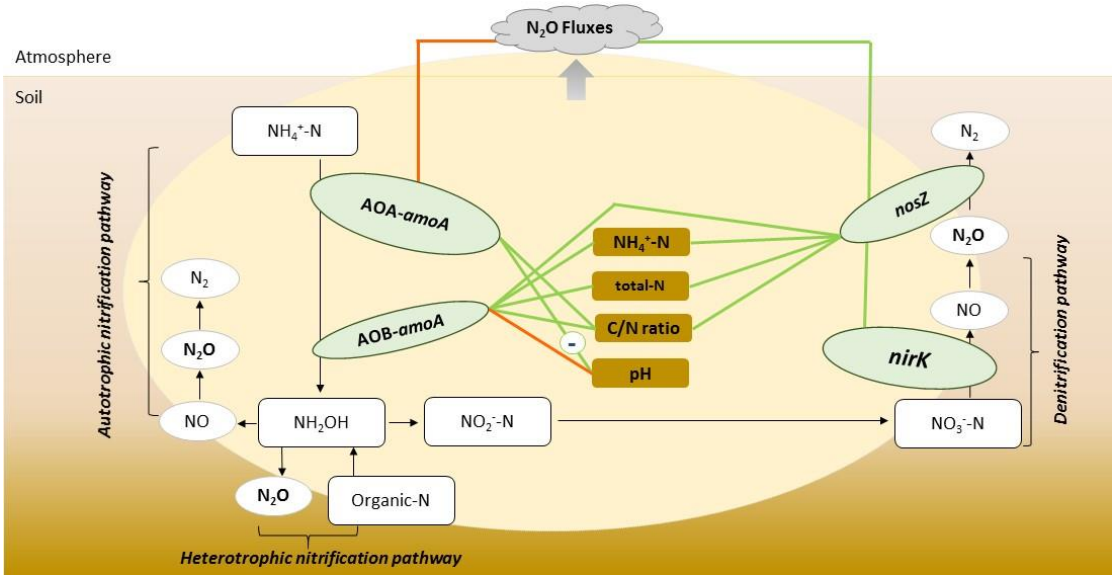


chinaXiv:201811.00111v1

chinaXiv:201811.00111v1

Supplementary information:

**Table S1** Primer information of selected soil functional genes.

| Gene | Primers | Primer sequence (5'--3') | Location | Length | References |
|---|---|---|---|---|---|
| AOB-*amoA* | amoA 1F | 5' GGGGTTTCTACTGGTGGT 3' | 322-249 | 500bp | (Rich et al., 2003; Levy-Booth et al., 2014) |
| | amoA 2R | 5' CCCCTCKGSAAAGCCTTCTTC 3' | 802-822 | | |
| AOA-*amoA* | CrenamoA 23F | 5' ATGGTCTGGCTWAGACG 3' | 7-24 | 620bp | (Levy-Booth et al., 2014) |
| | CrenamoA 616R | 5' GCCATCCATCTGTATGTCCA 3' | 611-631 | | |
| *nirK* | nirK F560-589 | 5'- GGGCATGAACGGCGCGCTCATGGTGCTGCC -3' | 560-589 | 376bp | (Levy-Booth et al., 2014) |
| | nirK R906-935 | 5'-CGGGTTGGCGAACTTGCCGGTGGTCCAGAC -3' | 906-935 | | |
| *nosZ* | nosZ-F | 5'- CGCTGTTCITCGACAGYCAG -3' | 1181-1201 | 700bp | (Rich et al., 2003) |
| | nosZ-R | 5'- ATGTGCAKIGCRTGGCAGAA -3' | 1880-1900 | | |

**Table S2** Reaction programs of quantitative PCR for selected functional genes.

| Gene | Primers | Thermal cycling conditions | References |
|---|---|---|---|
| AOB-*amoA* | amoA 1F<br>amoA 2R | 95° 30"-40(95° 15"-53° 15"-72° 40") | (Rich et al., 2003; Levy-Booth et al., 2014) |
| AOA-*amoA* | CrenamoA23F<br>CrenamoA616R | 95° 30"-40(95° 5"-53° 34"-72° 60") | (Levy-Booth et al., 2014) |
| *nirK* | nirK F560-589<br>nirK R906-935 | 95° 30"-40(95° 5"-65° 34"-72° 60") | (Levy-Booth et al., 2014) |
| *nosZ* | nosZ-F<br>nosZ-R | 95° 30"-40(95° 5"-56° 34"-72° 40") | (Rich et al., 2003) |

chinaXiv:201811.00111v1

chinaXiv:201811.00111v1

**Table S3** Soil physiochemical properties (average ± standard error in bracket, n = 3) before the tracing incubation. SC, SL, SM and SH indicate control, low-N, medium-N and high-N treatments in the short-term N addition site, respectively. LC, LL, LM and LH indicate control, low-N, medium-N and high-N treatments in the long-term N addition site, respectively. Same lowercase letters following each values indicate insignificant differences ($p > 0.05$) among different N-treatments of the short-term or long-term site.

| Site | Treatment | N-adding content | pH | $NH_4^+$-N | $NO_3^-$-N | TOC | Total N | C/N ratio | MBC | MBN |
|---|---|---|---|---|---|---|---|---|---|---|
| | | kg N $ha^{-1}$ $a^{-1}$ | | mg $kg^{-1}$ | | g $kg^{-1}$ | | | mg $kg^{-1}$ | |
| ***Short-term*** | **SC** | **0** | 3.90(0.03)$^{a}$ | 4.4(2.2)$^{a}$ | 7.1(1.7)$^{a}$ | 25.5(3.3)$^{b}$ | 1.9(0.1)$^{a}$ | 13.6(0.5)$^{a}$ | 300.4(87.8)$^{a}$ | 40.0(18.6)$^{a}$ |
| | **SL** | **35** | 3.90(0.01)$^{a}$ | 6.7(3.5)$^{a}$ | 7.5(0.7)$^{a}$ | 25.8(4.7)$^{b}$ | 1.7(0.4)$^{a}$ | 15.3(0.6)$^{a}$ | 138.8(42.8)$^{b}$ | 20.8(15.8)$^{a}$ |
| | **SM** | **70** | 3.84(0.02)$^{ab}$ | 6.0(1.2)$^{a}$ | 7.0(1.9)$^{a}$ | 25.7(1.7)$^{b}$ | 2.0(0.5)$^{a}$ | 13.3(1.4)$^{a}$ | 136.2(47.3)$^{b}$ | 17.0(2.9)$^{a}$ |
| | **SH** | **105** | 3.80(0.02)$^{b}$ | 3.0(1.2)$^{a}$ | 9.6(0.8)$^{a}$ | 27.6(2.9)$^{ab}$ | 1.9(0.3)$^{a}$ | 14.7(0.6)$^{a}$ | 192.0(14.3)$^{ab}$ | 18.5(0.7)$^{a}$ |
| ***Long-term*** | **LC** | **0** | 3.88(0.03)$^{a}$ | 5.9(3.5)$^{a}$ | 7.1(3.1)$^{a}$ | 26.8(2.2)$^{ab}$ | 2.0(0.1)$^{a}$ | 13.5(0.3)$^{a}$ | 290.7(127.4)$^{a}$ | 27.2(17.5)$^{a}$ |
| | **LL** | **50** | 3.82(0.04)$^{b}$ | 6.0(3.9)$^{a}$ | 8.1(4.5)$^{a}$ | 28.8(8.5)$^{ab}$ | 2.0(0.6)$^{a}$ | 14.3(0.1)$^{a}$ | 205.6(64.9)$^{ab}$ | 18.6(4.2)$^{a}$ |
| | **LM** | **100** | 3.71(0.04)$^{c}$ | 4.4(2.9)$^{a}$ | 9.3(1.6)$^{a}$ | 35.6(8.2)$^{a}$ | 2.4(0.4)$^{a}$ | 14.7(1.0)$^{a}$ | 296.0(61.3)$^{a}$ | 35.6(12.7)$^{a}$ |
| | **LH** | **150** | 3.67(0.07)$^{c}$ | 7.5(3.1)$^{a}$ | 10.0(2.8)$^{a}$ | 31.2(0.2)$^{ab}$ | 2.3(0.2)$^{a}$ | 13.8(0.7)$^{a}$ | 236.8(54.1)$^{ab}$ | 20.3(3.9)$^{a}$ |

**Table S4** Gross N transformation rates (average ± standard deviation in bracket) during the incubation of 8 N-treatments. Kinetics: 0 = zero-order, 1= first-order; $LSD_S$ or $LSD_L$: least significant difference when comparing any two means in the short-term or the long-term site for $p = 0.05$. Rates are in mg N $kg^{-1}$ $d^{-1}$. Detailed explanation of the N rates are as follows: $\boldsymbol{M_{Nrec}}$: mineralization of recalcitrant organic nitrogen to $NH_4^+$; $\boldsymbol{I_{NH4\text{-}Nrec}}$: immobilization of $NH_4^+$ to recalcitrant organic nitrogen; $\boldsymbol{M_{Nlab}}$: mineralization of labile organic nitrogen; $\boldsymbol{I_{NH4\text{-}Nlab}}$: immobilization of $NH_4^+$ to labile organic nitrogen; $\boldsymbol{O_{Nrec}}$: oxidation of recalcitrant organic nitrogen to $NO_3^-$; $\boldsymbol{I_{NO3}}$: immobilization of $NO_3^-$ to recalcitrant organic N; $\boldsymbol{O_{NH4}}$: oxidation of $NH_4^+$ to $NO_3^-$; $\boldsymbol{D_{NO3}}$: dissimilatory $NO_3^-$ reduction to $NH_4^+$; $\boldsymbol{A_{NH4}}$: adsorption of $NH_4^+$ on cation exchange sites; $\boldsymbol{R_{NH4a}}$: release of $NH_4^+$ on cation exchange sites). $\boldsymbol{NET_{NH4aprod}}$: net $NH_4^+$ production; $\boldsymbol{NET_{NO3aprod}}$: net $NO_3^-$ production.

| | | Short-term | | | | | Long-term | | | | |
|---|---|---|---|---|---|---|---|---|---|---|---|
| **N rates** | **Kinetics** | **SC** | **SL** | **SM** | **SH** | **$LSD_S$** | **LC** | **LL** | **LM** | **LH** | **$LSD_L$** |
| $\boldsymbol{M_{Nrec}}$ | 0 | 1.3(0.3)E-01 | 0.7(0.3)E-01 | 1.1(0.4)E-01 | 1.1(0.3)E-01 | *0.031* | 0.6(0.2)E-01 | 0.9(0.5)E-01 | 1.1(0.4)E-01 | 1.4(0.7)E-01 | *0.046* |
| $\boldsymbol{I_{NH4\text{-}Nrec}}$ | 1 | 5.8(3.7)E-03 | 2.7(1.5)E-03 | 6.4(4.4)E-03 | 4.2(2.4)E-03 | *0.003* | 4.4(1.5)E-03 | 3.3(1.1)E-03 | 6.2(3.6)E-03 | 1.1(0.5)E-01 | *0.026* |
| $\boldsymbol{M_{Nlab}}$ | 1 | 4.6(2.5)E-02 | 8.4(2.9)E-02 | 1.1(0.4)E-01 | 7.2(3.7)E-02 | *0.032* | 1.3(0.3)E-01 | 7.4(4.3)E-02 | 1.1(0.5)E-01 | 7.0(6.1)E-02 | *0.043* |
| $\boldsymbol{I_{NH4\text{-}Nlab}}$ | 1 | 7.5(2.7)E-03 | 2.8(1.5)E-03 | 4.5(2.8)E-03 | 5.7(3.3)E-03 | *0.002* | 3.4(0.9)E-03 | 2.0(0.6E-03) | 5.0(3.7)E-03 | 1.4(0.4)E-01 | *0.020* |
| $\boldsymbol{O_{Nrec}}$ | 0 | 1.0(0.9)E-05 | 1.5(1.0)E-05 | 1.2(1.1)E-05 | 1.0(0.6)E-05 | *8.6E-06* | 2.2(0.7)E-05 | 7.2(5.0)E-06 | 1.9(1.0)E-05 | 1.4(0.4)E-05 | *6.4E-06* |
| $\boldsymbol{I_{NO3}}$ | 1 | 3.8(4.9)E-03 | 2.5(1.8)E-02 | 1.8(1.1)E-02 | 1.1(0.9)E-02 | *0.011* | 3.0(1.6)E-02 | 8.0(7.5)E-03 | 5.2(1.4)E-02 | 5.0(4.0)E-03 | *0.011* |
| $\boldsymbol{O_{NH4}}$ | 1 | 1.8(0.1)E-01 | 1.9(0.2)E-01 | 1.6(0.2)E-01 | 1.8(0.2)E-01 | *0.017* | 1.7(0.0)E-01 | 1.6(0.2)E-01 | 1.8(0.2)E-01 | 8.0(0.8)E-02 | *0.014* |
| $\boldsymbol{D_{NO3}}$ | 1 | 3.4(1.6)E-03 | 1.6(0.1)E-02 | 1.2(0.2)E-02 | 5.0(1.2)E-03 | *0.001* | 6.0(0.8)E-03 | 7.0(1.3)E-03 | 4.5(2.1)E-03 | 6.9(1.3)E-03 | *0.001* |
| $\boldsymbol{A_{NH4}}$ | 1 | 1.4(0.5)E-02 | 5.7(6.1)E-03 | 1.1(0.5)E-02 | 1.6(0.8)E-02 | *0.006* | 1.4(0.4)E-02 | 1.2(0.8)E-02 | 2.6(0.5)E-02 | 1.0(0.6)E-02 | *0.005* |
| $\boldsymbol{R_{NH4a}}$ | 1 | 1.5(0.4)E-04 | 5.3(1.9)E-05 | 7.7(7.0)E-05 | 1.4(1.2)E-04 | *6.8E-05* | 1.1(0.7)E-04 | 8.4(3.4)E-05 | 2.7(0.7)E-04 | 1.3(0.4)E-04 | *5.2E-05* |
| $\boldsymbol{NET_{NH4+\ prod}}$ | | -2.6(3.0)E-03 | -3.1(2.9)E-02 | 5.4(5.7)E-02 | -1.9(3.4)E-02 | *0.092* | 2.2(3.6)E-02 | -3.4(0.4)E-03 | 8.3(0.6)E-03 | -1.3(0.3)E-01 | *0.144* |
| $\boldsymbol{NET_{NO3-\ Prod}}$ | | 1.7(0.0)E-01 | 1.5(0.0)E-01 | 1.3(0.0)E-01 | 1.7(0.1)E-01 | *0.029* | 1.4(0.1)E-01 | 1.4(0.1)E-01 | 1.2(0.1)E-01 | 6.9(0.2)E-02 | *0.025* |

chinaXiv:201811.00111v1

chinaXiv:201811.00111v1

**Figure legends**

**Fig. S1.** $^{15}N$ tracing model (Müller et al., 2007) (**$NH_4^+$**: ammonium; **$NH_4^+{}_{ads}$** : adsorbed $NH_4^+$; **$N_{lab}$**: labile organic N; **$NO_3^-$**: nitrate; **$N_{rec}$**: recalcitrant organic N. ***$M_{Nrec}$***: mineralization of recalcitrant organic nitrogen to $NH_4^+$; ***$I_{NH4\text{-}Nrec}$***: immobilization of $NH_4^+$ to recalcitrant organic nitrogen; ***$M_{Nlab}$***: mineralization of labile organic nitrogen; ***$I_{NH4\text{-}Nlab}$***: immobilization of $NH_4^+$ to labile organic nitrogen; ***$O_{Nrec}$***: oxidation of recalcitrant organic nitrogen to $NO_3^-$; ***$I_{NO3}$***: immobilization of $NO_3^-$ to recalcitrant organic N; ***$O_{NH4}$***: oxidation of $NH_4^+$ to $NO_3^-$ ; ***$D_{NO3}$***: dissimilatory $NO_3^-$ reduction to $NH_4^+$; ***$A_{NH4}$***: adsorption of $NH_4^+$ on cation exchange sites; ***$R_{NH4a}$***: release of $NH_4^+$ on cation exchange sites).

**Fig. S2.** The measured (scatters, average ± standard deviation, n = 3) and modeled (lines) N concentration (a, b, d, e) and $^{15}N$ enrichment (c, f) in inorganic-N of the eight N treatments during the incubation. Symbols (points and lines) in green and orange indicate the short-term and long-term N deposition treatments, respectively. SC, SL, SM and SH indicate control, low-N, medium-N and high-N treatments in the short-term site, respectively. LC, LL, LM and LH indicate control, low-N, medium-N and high-N treatments in the long-term site, respectively.

**Fig. S3.** Pearson correlation analysis results of soil properties, $N_2O$ fluxes, $N_2O$ emission proportions from ammonium ($^{15}N_2O/^{15}NH_4^+$) and nitrate pools ($^{15}N_2O/^{15}NO_3^-$), gene abundances, denitrification/nitrification ((*nirK* + *nosZ*)/(AOA-

*amoA* + AOB-*amoA*) ) and *nosZ*/*nirK* gene ratios in the short-term (a) and long-term sites (b). $N_2O_a$, $N_2O_h$ and $N_2O_d$ indicate different $N_2O$ fractions from autotrophic nitrification (a), heterotrophic nitrification (h) and denitrification (d) pathways, respectively. Squares in red, blue and yellow (light and medium) indicate $NH_4^+$-N, $NO_3^-$-N and organic-N pools (including $^{15}N$ labelled components coming from original isotopic addition solutions or from N transformation). Ovals in dark yellow and light green indicate soil properties and gene indicators (gene abundance and relative ratio), respectively. Overlaps in adjacent indicators indicate significant correlations, while insignificant correlations were not shown. There is no meanings for the size of the symbols mentioned in this figure. All the correlations mentioned in this figure are positively significant unless otherwise stated.

chinaXiv:201811.00111v1

**Fig. S1**

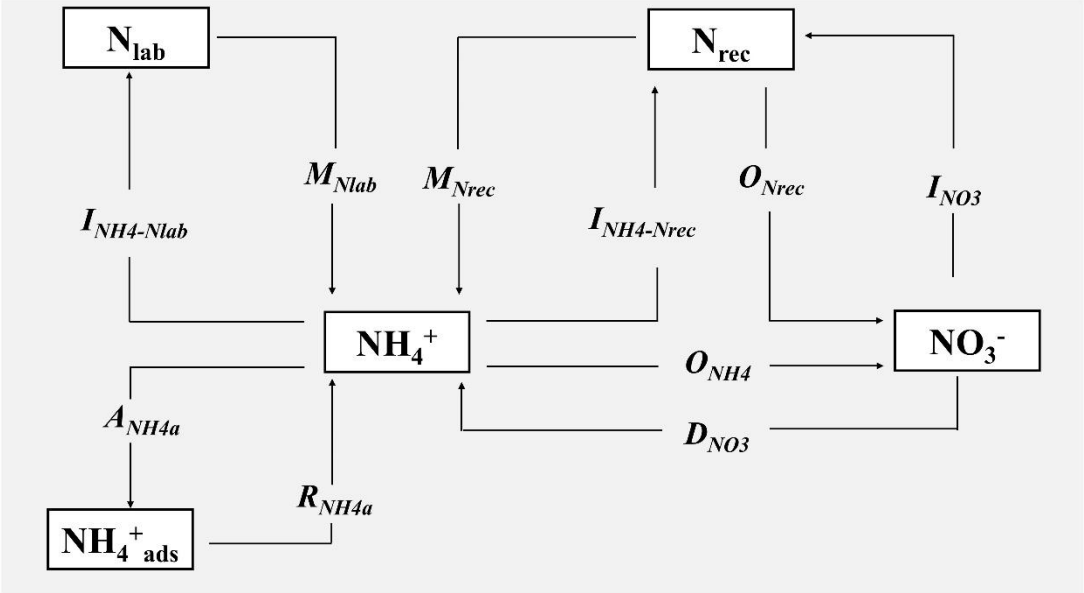


chinaXiv:201811.00111v1

**Fig. S2**

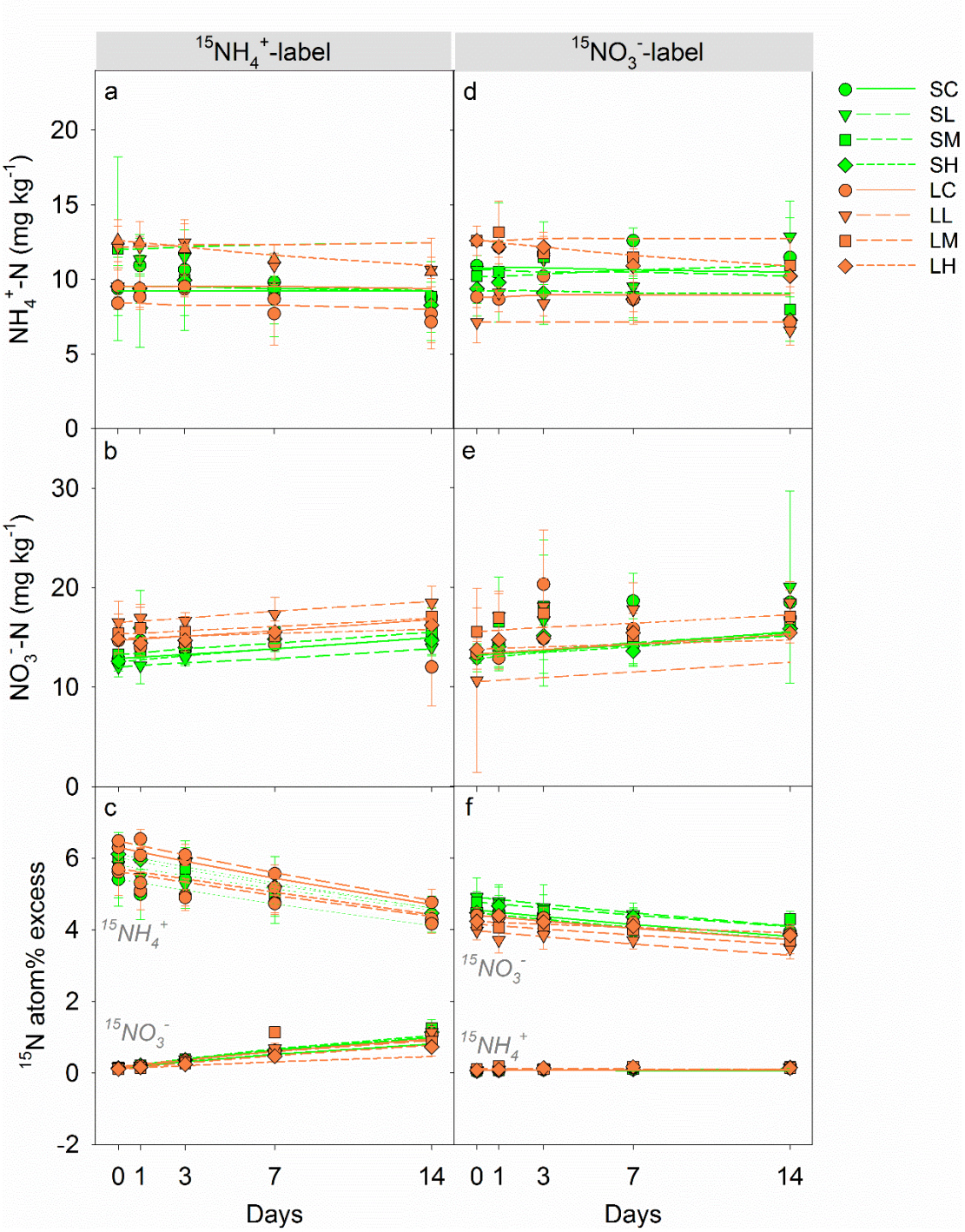


chinaXiv:201811.00111v1

chinaXiv:201811.00111v1

**Fig. S3**